Journal of Materials Chemistry B

ROYAL SOCIETY OF CHEMISTRY

REVIEW

View Article Online
View Journal | View Issue

Cite this: J. Mater. Chem. B, 2022, 10, 9314

Getting drugs to the brain: advances and prospects of organic nanoparticle delivery systems for assisting drugs to cross the blood–brain barrier

Qiuxia Tan,†[a] Shaojing Zhao,†[a] Ting Xu,[a] Qin Wang,[a] Minhuan Lan,*[a] Li Yan*[b] and Xianfeng Chen*[c]

Received 7th July 2022,
Accepted 27th September 2022

DOI: 10.1039/d2tb01440h

rsc.li/materials-b

The blood–brain barrier (BBB) plays an irreplaceable role in protecting the central nervous system (CNS) from bloodborne pathogens. However, the BBB complicates the treatment of CNS diseases because it prevents almost all therapeutic drugs from getting into the CNS. With the growing understanding of the physiological characteristics of the BBB and the development of nanotechnology, nanomaterial-based drug delivery systems have become promising tools for delivering drugs across the BBB to the CNS. Herein, we systematically summarize the recent progress in organic-nanoparticle delivery systems for treating CNS diseases and evaluate their mechanisms in overcoming the BBB with the aim to provide a comprehensive understanding of the advantages, disadvantages, and challenges of organic nanoparticles in delivering drugs across the BBB. This review may inspire new research ideas and directions for applying nanotechnology to treat CNS diseases.

1. Introduction

Central nervous system (CNS) diseases, such as brain tumors, Alzheimer's disease (AD), Parkinson's disease, and Huntington's disease, pose a tremendous threat to human health.[1,2] However, it is notoriously difficult to treat CNS diseases due to the presence of the blood–brain barrier (BBB) between the blood plasma and brain cells. The BBB is mainly composed of brain microvascular endothelial cells (BMECs), astrocytes, neuron end-feet, pericytes, resident microglia, and tight junctions;[3,4] among which, BMECs are attached closely to one another through tight connection to form the physical barrier of the brain. Astrocytes are responsible for maintaining the homeostasis,[5] and pericytes, which are partly wrapped by BMECs, are responsible for the permeability of the BBB.[6] These structural properties endow the BBB with selective permeability, allowing the passage of nutrients required by the brain tissue, but blocking that of harmful substances. Although the BBB plays a vital role in maintaining the physiological state of the CNS, it prevents many therapeutic drugs from entering the brain, thereby hindering the treatment of CNS diseases.[7,8] Usually, essential molecules and therapeutic agents cross the BBB *via* various mechanisms such as passive diffusion, receptor-mediated transport (RMT), carrier-mediated transport (CMT), adsorption-mediated transport (AMT) and cell-mediated transport (CET). Currently, the following method approaches are commonly used to increase the efficacy of drug delivery across the BBB; however, each approach has some disadvantages:

(1) Improving the lipid solubility of drugs. Changing the physicochemical properties of drugs may reduce their pharmacological activity. In addition, the presence of P-glycoprotein (P-gp) in the cytomembrane can prevent these highly lipid-soluble drugs from entering the brain.

(2) Using P-gp inhibitors for highly lipid-soluble drugs. This approach can avoid the efflux of P-gp and promote the drug delivery into the brain;[9] however, inhibiting P-gp may also allow some harmful lipid-soluble compounds to enter the brain.

(3) Loosening of the tight junctions to open the BBB. In general, hypertonic solutions,[10] vasoactive substances, and focused ultrasound[11] can temporarily and reversibly open the BBB; however, this approach is non-specific and may damage the endothelial cells and tissues of the brain. Moreover, the non-selective opening of the BBB may also allow harmful substances to enter and damage the brain.

[a] Hunan Provincial Key Laboratory of Micro & Nano Materials Interface Science, College of Chemistry and Chemical Engineering, Central South University, Changsha, 410083, China. E-mail: minhuanlan@csu.edu.cn
[b] College of Health Science and Environmental Engineering, Shenzhen Technology University, Shenzhen, 518118, China. E-mail: yanli@sztu.edu.cn
[c] School of Engineering, Institute for Bioengineering, University of Edinburgh, The King's Buildings, Edinburgh EH9 3JL, UK. E-mail: Michael.Chen@ed.ac.uk
† These authors contributed equally.

(4) Bypassing the BBB. Some invasive approaches (*e.g.*, intrathecal administration) and non-invasive approaches (*e.g.*, intranasal administration) are the commonly used BBB bypassing methods in treating CNS diseases. However, the intrathecal administration is highly invasive and causes patient discomfort,[12] whereas the intranasal administration suffers from limited dose, low nasal mucosa membrane permeability, and mucociliary clearance.[13]

By contrast, advanced strategies used to cross the BBB could realize the brain-targeted administration of drugs with minimal system toxicity, and minimal physical and chemical damage to the BBB. To date, a wide variety of drug delivery systems, including inorganic- and organic-based nanocarriers, have been developed.[14–16] However, inorganic-based nanocarriers, such as metal-, carbon-, and semiconductor-based nanomaterials, suffer from non-degradability and inherent cytotoxicity, which is the biggest limitation on the clinical transformation. Additionally, inorganic materials are more frequently used in imaging than carriers. In contrast, organic nanocarriers have the advantages of high biocompatibility, low toxicity, and easy modification and functionalization, thus are potential tools for delivering drugs across the BBB. In 2018, Furtado *et al.* systematically reviewed the anatomy, physiology, and pathology of the BBB, and summarized the approaches for bypassing or crossing the BBB. However, only a few sections in the article described the use of nanocarriers to cross the BBB.[17] In 2019, Xie *et al.* reviewed different delivery approaches for crossing the BBB, including intranasal delivery, temporary disruption of the BBB, local delivery, and receptor- or peptide-mediated BBB-crossing strategies.[18]

This field develops rapidly, and many new strategies are reported every year. One attractive approach in reviewing the extensive progress of the field is to categorize the designed strategies and functions based on the nanomaterials used in the applied drug delivery systems. Therefore, in this review, we summarize the recent progress in the development of various types of organic nanocarriers used to overcome the BBB, including lipid-based NPs (*i.e.*, liposomes, solid lipid NPs, and micelles), polymer-based NPs (*i.e.*, amphiphilic copolymers and dendrimers) and biomolecule-based NPs (*i.e.*, protein-, virus-, and nuclear-based NPs) (Scheme 1). The controllable preparation, functional surface modifications, drug loading and release kinetics, working mechanism, and therapeutic effects of these nanocarriers are described in detail. We also compare and discuss the advantages and disadvantages of these organic NPs, and highlight the significance of their physicochemical properties and biological functions (especially surface modifications) in contributing to the BBB-crossing. Lastly, we present our insights into the opportunities and challenges of NP-delivery systems in crossing the BBB for effective treatment of CNS diseases.

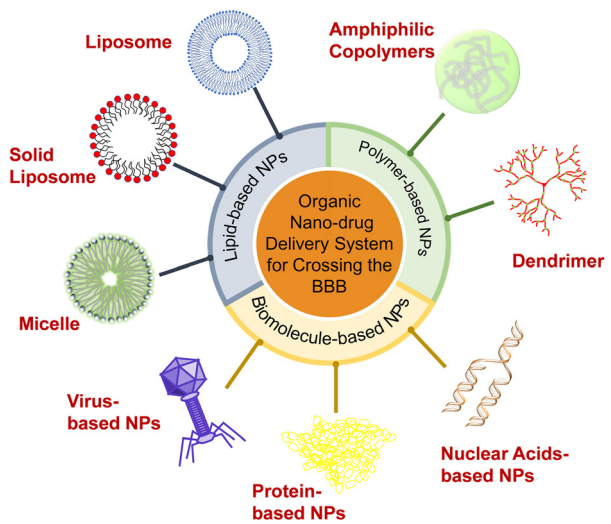

Scheme 1 Organic-nanoparticle (NP) delivery systems for crossing the blood–brain barrier.

2. Organic-NP delivery systems

Organic NPs, including lipid-, polymer-, and biomolecule-based NPs which can penetrate the BBB and deliver drugs to the CNS have been developed. After surface modification to improve surface charge, lipophilicity, biocompatibility, and brain targeting ability, these organic NPs can avoid phagocytosis by the reticuloendothelial system (RES) and significantly increase the concentration of drugs in the brain. For example, decorating with polyethylene glycol (PEG) can prolong the retention time of liposomes in blood. Targeting ligands allow NPs to get through the BBB with different transport mechanisms and realize active targeting to promote the carriers to further accumulate in the brain. Furthermore, modification of surfactants can alter the surface charge and improve the BBB-crossing by the enhanced electrostatic interaction.

2.1. Lipid-based NPs

2.1.1 Liposomes. Liposomes are bilayer vesicles formed by amphiphilic phospholipids with extensive use in drug delivery because of the following advantages. (1) High adaptability to loaded drugs: hydrophilic and hydrophobic drugs are loaded into the water phase and the lipid membrane, respectively, and the amphiphilic drugs are located between the phases (Fig. 1A). Thus, liposomes can simultaneously carry both hydrophilic and hydrophobic drugs, while protecting them from being diluted by body fluids and destroyed by enzymes in the body.[19] (2) Good biocompatibility and high bioavailability: phospholipids are cell-membrane components that do not elicit toxicity upon injection into the body with a low immune response.[20] The electrostatic interaction between the surface charge of cationic liposomes and the negatively charged BBB can trigger the cellular internalization of liposomes, thereby effectively promoting liposomes to get into the brain.[21] In addition to the decoration with PEG and active targeting ligands, embellishment of some cellular membrane proteins can camouflage the surface of nanocarriers to acquire homologous targeting and immune-escaping characteristics. The interaction between tumor cell-membrane proteins and their receptors on cells can realize

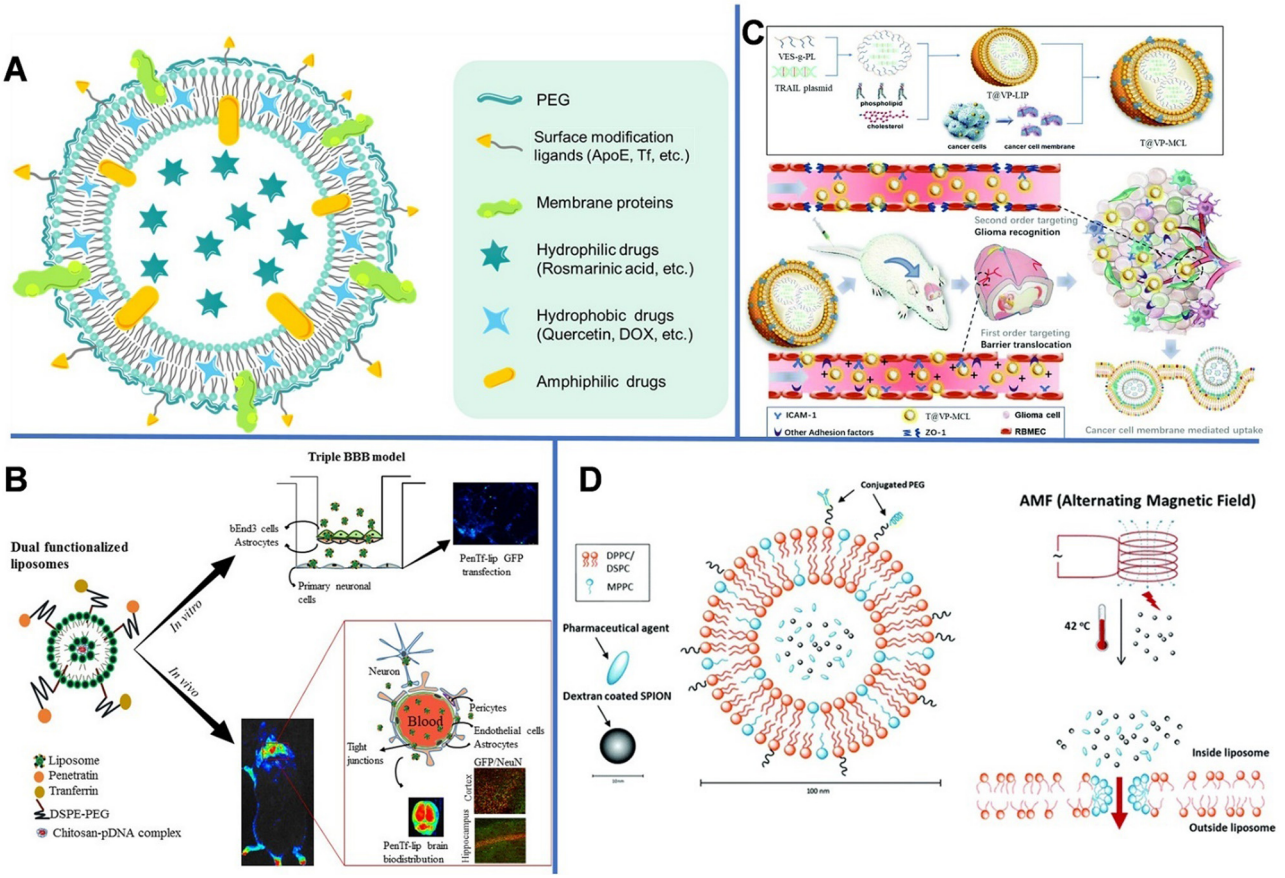

Fig. 1 (A) Schematic diagram of the drug-loading liposome. (B) Gene delivery mediated by bifunctional liposomes. Reprinted with permission from ref. 29. Copyright 2018, Elsevier. (C) Tumor cell-membrane modified liposomes were used to specifically target homologous glioma and cross the BBB. Reprinted with permission from ref. 31. Copyright 2020, Royal Society of Chemistry. (D) Magnetic-field mediated drug release from micelles. Reprinted with permission from ref. 35. Copyright 2019, Royal Society of Chemistry.

self-recognition of the biomimetic nanoparticles. These multi-functional liposomes combined with other processes to open the BBB can further promote the dug-delivery system to get into the brain for improved diagnosis and treatment. Some other types of liposomes, such as temperature-sensitive liposomes, have a controlled drug release ability in the brain, thus can reduce the risk of pre-leakage.

However, conventional liposomes can be easily removed by the RES, leading to rapid systematic clearance. Liposomes modified with hydrophilic PEG can avoid being captured by the RES, thereby increasing the drug uptake in the brain.[22] Xie *et al.* modified liposomes with glucose (Glu) and PEG with various chain lengths (PEG200, PEG400, PEG1000, and PEG2000) and demonstrated that the PEG length has a great impact on the brain-targeting efficiency of the liposomes,[23] and PEG1000-modified liposomes exhibited the most outstanding brain-targeting ability. This is likely because short PEG chains can block the exposure of Glu, which helped the transport of liposomes into the brain by RMT through the multivalent recognition between glucose transporter-1 (GLUT1) in the brain capillary endothelial cells and Glu,[24] whereas long PEG chains provided steric hindrance. Zhang *et al.* prepared a PEGylated liposome modified with a cell penetration peptide (CB5005) containing DOX.[25] The prepared liposomes had regular sphere shapes with a diameter of approximately 110 nm. The dual functions of CB5005, namely cell membrane penetration function and nuclear factor-κB (NF-κB) inhibition functions, could effectively penetrate gliomas and inhibit the activation of NF-κB. The modification with CB5005 not only significantly increased the uptake of liposomes by glioma cells, but also greatly improved the killing effect of DOX on U87 tumor cells.

Conjugating liposomes with brain-specific ligands or antibodies can improve the targetability and promote the nanodrugs getting into the brain by RMT. For example, apolipoprotein E (ApoE) can bind to receptors (low-density lipoprotein receptors (LDLRs)) and LDLR-related proteins (LRPs) on the BBB. Transferrin (Tf) is a glycoprotein that can transport iron ions into cells.[26] Cheng *et al.* developed Tf-modified and PEGylated liposomes to encapsulate chemotherapeutic osthole (Ost) (Tf-Ost-Lip) to treat AD.[27] Muzykantov *et al.* constructed vascular cell adhesion molecule 1 (anti-VCAM)-conjugated liposomes, which exhibited improved brain accumulation compared to TfR or intercellular adhesion molecule 1 (ICAM-1)-conjugated liposomes. The uptake efficiency of intravenously injected anti-VCAM-liposomes in an

inflamed brain was 27-fold and 8-fold greater than that of TfR-1- and ICAM-1-liposomes, respectively, achieving a brain/blood ratio >300-fold higher than that of immunoglobulin G/liposomes.[28]

However, RMT is a transport process that can usually become saturated. Dual targeting is one of the fascinating strategies for overcoming the receptor saturation and increasing the delivery efficiency. In 2018, Rodrigues *et al.* designed liposomes (penetratin [Pen]-Tf liposomes) with dual targeting functions to achieve neuronal transfection, in which Tf could cross the BBB, while the cationic cell-penetrating peptide (Pen) could overcome the receptor saturation and promote the intracellular delivery and endosomal escape.[29] The obtained liposomes were spherical with uniform particle sizes of 147–167 nm. Subsequently, the hydrophilic plasmid formed by complexing galactosidase with chitosan was encapsulated in liposomes, in which chitosan could keep DNA from enzymatic degradation and improve its transfection efficiency (Fig. 1B). The encapsulation efficiency of plasmid DNA (pDNA) encoding green fluorescent protein in the liposomes reached up to 93%. *In vitro* experiments revealed that after 8 h, 15.2% of Pen-Tf liposomes could cross the BBB, which is higher than that of Pen (2.6%) and Tf (3.5%) liposomes.

In the following years, the same research group used liposomes modified with dual targeting molecules (Tf and Pen) to deliver DOX and erlotinib to the brain. Results showed that the accumulation of DOX and erlotinib in the mouse brain increased by 12 fold and 3.3 fold, respectively, by using Tf-Pen liposomes. In addition, mice had a longer survival time and smaller glioblastoma in the brain compared with the control group, demonstrating the excellent anti-tumor effects of Tf-Pen liposomes, as well as its potential in the treatment of aggressive gliomas.[30]

Unlike the complex ligand modification process, liposomes provide an easy route to use cellular membrane proteins to camouflage the surface of nanocarriers. As shown in Fig. 1C, vitamin E succinate-grafted ε-polylysine (VES-*g*-PL) polymers could assemble into cationic micelles which were used to condense tumor necrosis factor-related apoptosis-inducing ligand plasmids. The VES-*g*-PL micelles and the glioma cell membrane were encapsulated in the inner compartment of the liposomes (egg lecithin and cholesterol) and the lipid layer, respectively. This led to the formation of T@VP-MCL with spherical morphology ($\sim$130 nm) and a zeta potential of 14.9 mV.[31] The electrostatic adsorption between the liposomes and endothelial cells increases the penetration efficiency of NPs. In addition, the liposomes can target ICAM-1 in gliomas to regulate the expression of the tight junction protein ZO-1. As can be seen in the magnetic resonance images, the tumor volume of rats in the control groups gradually increased over time, whereas that of rats in the experimental group showed relatively slower tumor growth.

A combination of low-intensity pulsed focused ultrasound (LIFU) with systemically administered microbubbles could generate mechanical stress to the brain endothelium to reversibly open the BBB. It has been reported that image-guided LIFU has been used to deliver stable liposomal *O*6-(4-bromothenyl) guanine (*O*6BTG) derivative. Liposomes can be used as pseudo-substrates to target *O*6-methylguanine-DNA methyltransferase (MGMT), an enzyme capable of repairing temozolomide-induced toxic DNA, thus leading to MGMT depletion to overcome MGMT-mediated chemotherapeutic drug temozolomide resistance. Compared with that in the untreated area of the contralateral hemisphere, the accumulation level of dye-labeled liposomes in the LIFU-treated area was significantly higher.[32] In addition, Lin *et al.* prepared a gene delivery system, in which gene-carrying liposomes were combined with microbubbles and ultrasound was used to open the BBB to deliver glia-cell-line-derived neurotrophic factor and brain-derived neurotrophic factor (therapeutic genes commonly tested in Parkinson's disease gene therapy) to the brain.[33] The results indicated that the ultrasound helped to open the BBB and increase the penetration of drugs and genes into the brain tissue for the treatment of CNS diseases.

Other than enhanced drug delivery, temperature-sensitive liposomes (TSL) can be used in controlled drug release under thermal stimulation, owing to their phase-change ability at a high temperature. When the temperature reaches the phase-transition temperature (usually >40 °C), liposomes collapse and release encapsulated drugs. The TSLs utilize the intravascular triggered wrapped drug release, in which the drug is released while liposomes are transiting through heated tissue. Some TSL formulations can release drugs within seconds. The higher the temperature or the longer the heating time, the more rapid the drug release. Since the heat stimulation is also helpful to open the BBB, TSL can cross the temporarily disrupted area of the BBB and reach the brain tissue.[34] Shi *et al.* developed a dual-function temperature-sensitive liposome system to encapsulate drugs.[35] Therein, glioblastoma multiforme (GBM)-specific cell-penetrating peptide and anti-GBM antibody were coupled to the outer layer of liposomes for targeted delivery. Then, superparamagnetic iron oxide NPs (SPIONs) and DOX were loaded into the liposomes. The alternating magnetic field could induce the SPIONs to generate heat, which subsequently triggered the release of DOX (Fig. 1D). Compared with non-functionalized liposomes, the dual-function liposomes could better enter U-87 human GBM cells and inhibit the proliferation of tumor cells; nonetheless, they had no major effect on the function of healthy brain cells.

The above examples demonstrate that encapsulating drugs into liposomes can prolong the half-life in the blood circulation, reduce side effects, and enhance the therapeutic effects on CNS diseases. However, physical, chemical, and biological factors, such as temperature, phospholipid materials, solvent properties, preparation methods, and stirring speed during the preparation, storage, and application processes can also affect the liposome structure. Thus, these factors directly affect the drug-carrying stability and biological functions of liposomes and need to be further studied before their clinical applications.

2.1.2 Solid lipid NPs. SLNs are solid colloidal particles consisting of natural or synthetic solid lipids, such as lecithin and triacylglycerol that can encapsulate or embed drugs into the lipid core.[36] SLNs can improve the physical and chemical

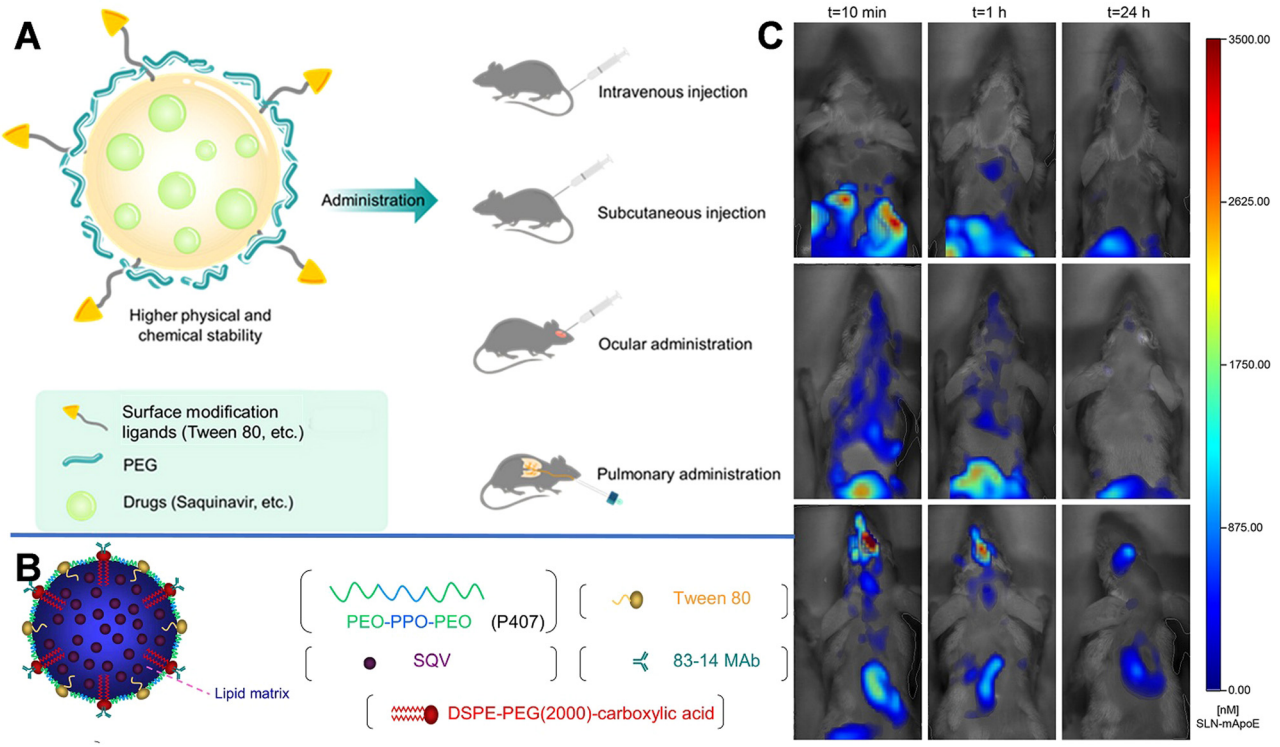

Fig. 2 (A) Schematic diagram of SLN and the multiple administrations. (B) Schematic structure of an 83–14 MAb/SQV-SLN. Reprinted with permission from ref. 39. Copyright 2013, Elsevier. (C) Biodistribution of DiR-loaded SLN-mApoE in mice. Reprinted with permission from ref. 42. Copyright 2017, Elsevier.

stability of drugs, prevent drug degradation, bypass efflux transporters (such as P-gp), enhance the brain-targeting ability of drugs, and accommodate the slow release of drugs. Decoration with surfactants can improve the stability of SLNs, and certain surfactants can inhibit P-gp, thereby promoting the accumulation of drugs in the brain. Compared with liposomes, SLNs have higher physical and chemical stability. SLNs are compatible with multiple administration routes, including intravenous injection, subcutaneous injection,[37] ocular administration, and pulmonary administration[38] (Fig. 2A). Kuo *et al.* prepared SLNs with 83–14 monoclonal antibody modified to load saquinavir (SQV) modified with the 83–14 monoclonal antibody (Fig. 2B).[39] The outer layer was coated with surfactant poloxamer 407 (P407, PEO–PPO–PEO) and polysorbate 80 (Tween 80) containing abundant PEO groups to improve metabolic stability and brain accumulation before being modified with DSPE-PEG2000. The 83–14 monoclonal antibody can selectively bind to the α-subunit of the human insulin receptor and therefore can serve as a brain-targeting vector. Tween 80 could adsorb apolipoprotein E from blood plasma onto the NPs surface to mimic low-density lipoprotein (LDL) that can be recognized by LDLRs; this allowed the NPs to enter the brain endothelial cells through RMT. In addition, Tween 80 inhibited the efflux function of P-gp on human brain microvascular endothelial cells (HBMECs). Collectively, SQV-SLNs modified with the 83–14 monoclonal antibody and Tween 80 could stimulate endocytosis and promote the entry of SLNs into HBMECs.

Furthermore, using Compritol 888 ATO (a mixture of mono-, di-, and tri-glycerides of behenic acid) as the solid lipid and Brij 78 (polyoxyethylene 20 stearyl ether derived from stearic-acid molecules covalently conjugated to PEG 1000) as a surfactant, Graverini *et al.* prepared SLNs *via* an emulsification/evaporation/solidification method to encapsulate andrographolide (AG) with an efficiency of 92%.[40] The prepared SLNs were spherical with a diameter of 300 nm. And Brij 78 in the SLNs could reduce opsonization, phagocytosis, and clearance by the liver and RES, while protecting NPs from interference of plasma, and prolonging their half-life in the blood circulation. Furthermore, the formulation was highly lipophilic and charged, thus could protect NPs from astrocyte and pericyte attacks and facilitate the permeation of drugs across the neurovascular junction. After incubating the hCMEC/D3 cell monolayer with NaF and 80 μM AG-loaded SLNs for 1 h, the permeability reached $26.8 \pm 4.17 \times 10^{-6}$ cm s^{-1}, which was approximately 3-fold higher than that of free AG.

Decoration with bioactive molecules can also facilitate the BBB-crossing ability. For example, Bozkir *et al.* used ApoE modification to improve the BBB permeability of donepezil and rhodamine B-loaded liposomes (ApoE-DON-SLNs). After 2 h of incubation, the uptake of ApoE-DON-SLNs by endothelial cells increased by over 4 fold higher than that of non-targeting liposomes.[41] SLNs with ApoE-derived peptide (SLN-mApoE) as a specific brain-targeting ligand were also prepared *via* warm micro-emulsification technology. Magro *et al.* investigated the

effects of various administration methods (including intravenous, intraperitoneal, and pulmonary administrations) on the bioavailability of SLN-mApoE in the brain.[42] The biodistribution of SLN-mApoE was subsequently evaluated at different times. As shown in Fig. 2C, after intraperitoneal injection, the abdominal cavity exhibited strong fluorescence originating from SLN-mApoE, whereas the brain was dark. The percentage of the fluorescence signals in the brain were 0.15% and 0.06% of the injected dose at 3 and 24 h after intravenous injection of SLN-mApoE, respectively. In contrast, the pulmonary administration of SLN-mApoE did not cause an acute inflammatory response in the lungs.

2.1.3 Micelles. Micelles have a spherical core–shell structure formed by self-assembly of amphipathic surfactants in water, which are the commonly used nanocarriers for brain-targeted NP-delivery systems, owing to their advantages of stable thermodynamics, good biocompatibility, and easy preparation. In general, micelles contain a hydrophobic core that can be used to load insoluble drugs and a hydrophilic shell that can protect the loaded drugs against environmental damage and prolong their retention time in blood circulation.[43,44] Additionally, some tumor microenvironment-responsible linkers are used to construct nanocarriers, thus realizing tumor-specific release of encapsulated drugs (Fig. 3).

Vasudevan *et al.* synthesized stearic acid (SA)-modified glycol chitosan (GC) (SAGC) that could spontaneously form spherical core–shell-structured micelles with a diameter of 138 nm in an aqueous solution (Fig. 4A).[45] The SA component formed a hydrophobic core to help hold the drug (curcumin, Cur) with a loading efficiency of 76%. The GC component formed the surrounding hydrophilic corona and aids in water solubility. The micelles were further modified with a targeting peptide (TGN peptide-TGNYKALHPHNG) to enhance the BBB-crossing capability. The obtained micelles (TSAGC) could effectively encapsulate Cur (a hydrophobic drug) and deliver it to the brain. *In vivo* experiments showed that the accumulation of TSAGC in the brain is higher compared with that of SAGC at 1 h post-injection, confirming the TGN peptide-mediated delivery.

Singh *et al.* prepared biocompatible multifunctional theranostic and photonic NPs (TPNs) that could cross the BBB and be tracked after systemic administration (Fig. 4B).[46] In this work, the TPNs were 20 nm ultra-small nano-micelles (TPN-Cur/encapsulating photonic molecule [CbV]) with a spherical shape, assembled by pluronic (F-127, PEO–PPO–PEO), Cur, and CbV. F-127 could bind to the plasma membrane to enhance the endocytosis-mediated transendothelial migration by inhibiting the activity of P-gp or promoting the vesicular transport by the micellar structure. Besides, CbV exhibited strong solid-state fluorescence in the near-infrared region and could be used to enhance the optical signal of TPNs. In TPN-Cur/CbV micelles, the fluorescence of Cur was quenched by CbV through an energy transfer mechanism. However, after Cur was released from the micelles, its fluorescence was recovered. This mechanism could be used to monitor the *in vivo* release of Cur. *In vivo* imaging of temporal signals from TPNs revealed that the obtained TPN-Cur/CbV accumulated in the brain within 30 min, and the intensity reached the maximum at 2–3 h post-injection.

By conjugating camptothecin (CPT) to PEG through a disulfide bond, Lu *et al.* prepared a pro-drug and then modified it with the tumor-penetrating peptide (iRGD).[47] As shown in Fig. 4C, CPT–S–S–PEG–COOH-based spherical micelles with a diameter of about 100 nm could encapsulate photosensitizer IR780. The iRGD peptide enhanced the ability of NPs to target neural GBM cells through the αvβ-integrin- and neuropilin-1-mediated ligand-transport mechanisms. *In vivo* experiments revealed that iRGD-micelles started to accumulate in the brain at 30 min post-injection. In GBM cells, a high concentration of glutathione (GSH) broke the S–S bond, causing the release of CPT and IR780, recovering their potential of chemical and photodynamic therapies.

Antisense oligonucleotide (ASO), a widely used therapeutic agent to treat CNS diseases, is an artificially synthesized nucleic-acid fragment designed to bind to noncoding and toxic RNAs associated with disease pathogenesis.[48] Min *et al.* prepared ASO-loaded glucosylated-polyion complex micelles (Glu-PIC/M) with a sphere shape and a size of 40 nm, formed by self-assembly of ASO and a mixture of Glu-PEG-PLL (MPA/IM) and MeO-PEG-PLL (MPA/IM) (Fig. 4D).[49] PEG-PLL (MPA/IM) is a block copolymer consisting of poly(ethylene glycol)-*b*-poly(L-lysine), 3-mercaptopropyl amidine, and 2-thiolaneimine. The density of Glu in NPs could be regulated by adjusting the ratio of the two polymers, and ASO could be effectively wrapped inside the core of the micelle. The concentration of ASO-loaded Glu-PIC/Ms in the brain was significantly increased by the overexpressed Glu transporter-1 on brain capillary endothelial cells. Furthermore, disulfide crosslinking could be created in the PIC/M core. The disulfide bond in the micelles was cleaved in the reduced microenvironment of the brain, resulting in the release of the carried ASO. *In vivo* results showed that ASO was delivered to multiple areas of the brain parenchyma of glycemic-controlled fasting mice at 1 h after tail-vein injection. The optimized nanocarrier efficiently knocked out the long non-coding RNA target gene in different areas of the brain (including the cerebral cortex and hippocampus). These results prove that Glu-modified nanocarriers have great potential in minimally invasive implementation of ASO therapy.

Monosialohexylganglioside (GM1) is the main component of mammalian gangliosides and is mainly composed of hydrophilic sugar chains and lipophilic ceramide.[50] LysoGM1 is a

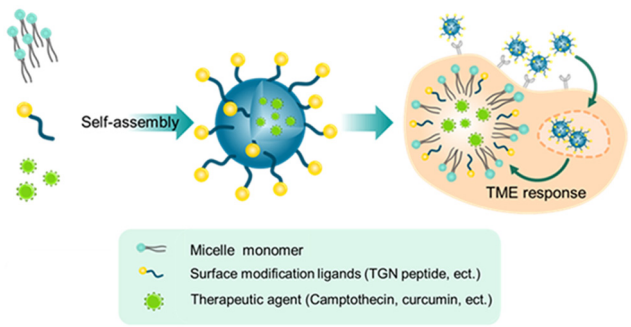

Fig. 3 Schematic illustration of drug-loading micelles.

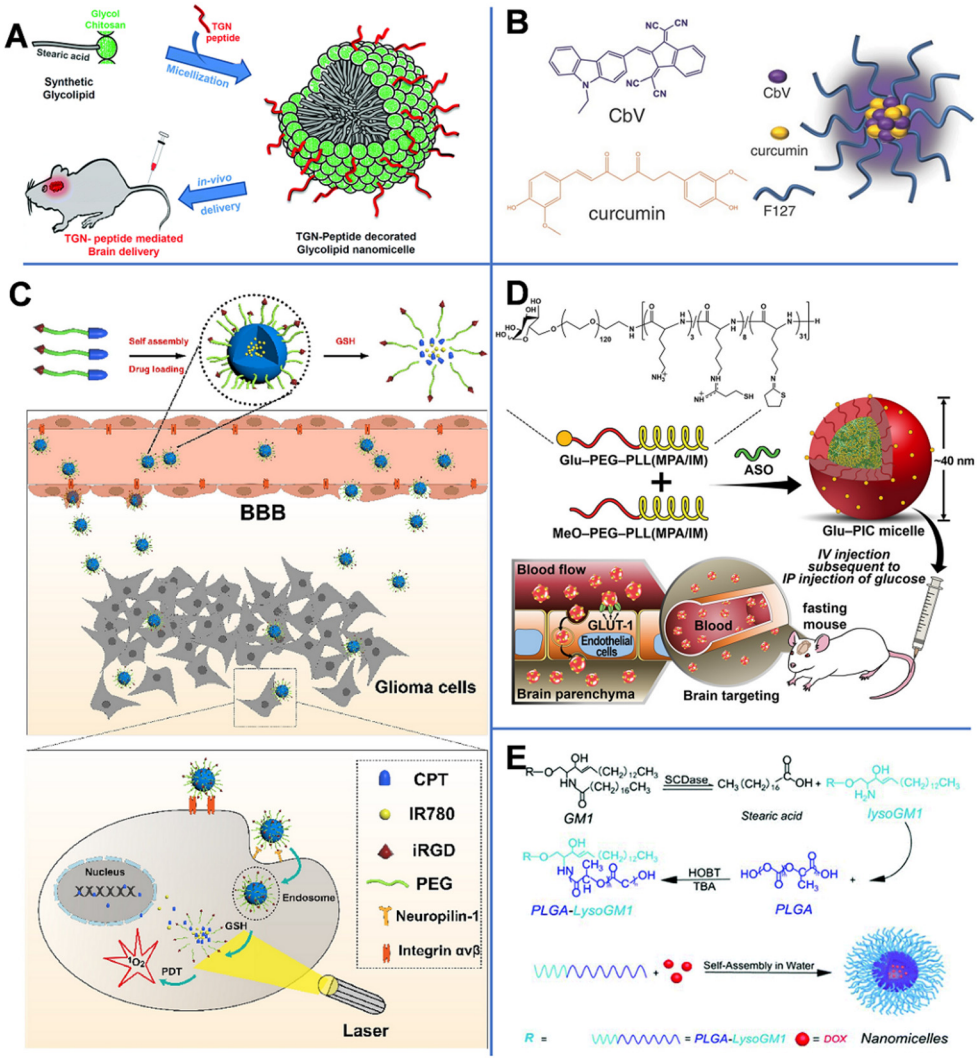

Fig. 4 (A) TGN-peptide-modified nano micelles. Reprinted with permission from ref. 45. Copyright 2019, Royal Society of Chemistry. (B) CbV- and Cur-based micelles. Reprinted with permission from ref. 46. Copyright 2016, Wiley-VCH. Schematic illustrations of (C) iRGD-peptide-modified micelles. Reprinted with permission from ref. 47. Copyright 2020, Elsevier. (D) ASO-loaded and Glu-modified micelles. Reprinted with permission from ref. 39. Copyright 2020, Wiley-VCH. (E) PLGA-lysoGM1/DOX micelles. Reprinted with permission from ref. 51. Copyright 2015, Elsevier.

hydrolyzed product of GM1. Yin *et al.* designed anticancer drug DOX-loaded poly(lactic-*co*-glycolic acid)-LysoGM1 (PLGA-LysoGM1) micelles with sustained and pH-sensitive drug release capacity (Fig. 4E) and proven that the PLGA-LysoGM1/DOX could effectively induce the apoptosis of drug-resistant GBM cells.[51] Transmission electron microscopy (TEM) results showed that the spherical PLGA-lysoGM1 and PLGA-lysoGM1/DOX micelles were 33.3 and 27.8 nm, respectively. *In vivo* studies were also conducted in zebrafish, mice, and rats. *In vivo* fluorescence imaging indicated that PLGA-lysoGM1/DOX micelles began to enter the brain of zebrafish at 20 min after intracardiac injection and enter the brain of mice at 1 h after intravenous injection. The results confirmed that the micelles could specifically accumulate in the brain to exert a significant anti-neural GBM effect on rats with intracranial nerve GBM.

In attempts to suppress oxidative stress, immune response, and microvascular dysfunction caused by reperfusion injury, Lu *et al.* designed rapamycin-encapsulated fibrin-binding polymer self-assembled micelles (CPLB/RAPA). Rapamycin can attenuate reperfusion injury. According to an *in vitro* simulation experiment, only the CPLB/RAPA experimental group could maintain the integrity of the BBB.[52] In the same year, the authors prepared a reactive oxygen species (ROS)-responsive polymer micellar system modified with a receptor for advanced glycation end-product (RAGE)-targeting peptide (Ab) derived from Aβ protein (Ab-PEG-LysB/Cur, [APLB/Cur]). These uniform sphere-like micelles with a diameter of 65 nm were found to accumulate at the diseased area *via* the Aβ-transportation-mimicked pathway and play a synergistic role in ROS clearance and Aβ inhibition under the stimulation by the microenvironment.[53]

2.2. Polymer-based NPs

Polymer-based NPs are formed by the assembly of polymers. According to the building blocks, polymer-based NPs can be

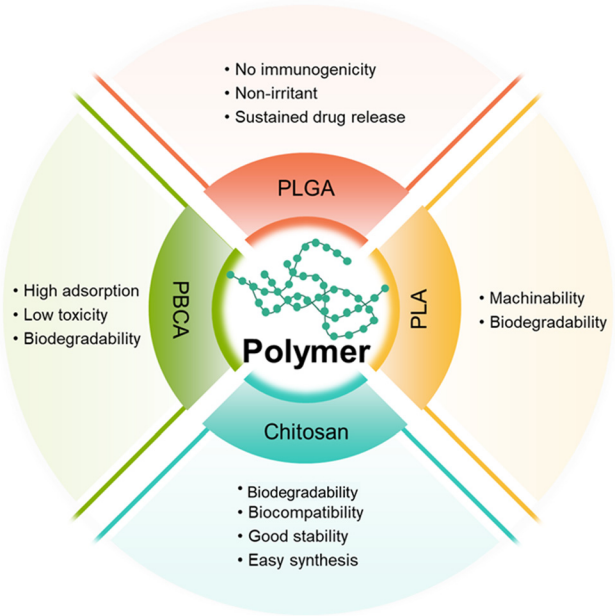

Fig. 5 Comparison of different types of amphiphilic copolymers.

divided into amphiphilic block copolymers and dendrimers. As a drug carrier, polymer-based NPs possess many advantages as follows: (1) the large molecular weight, which can to prolong the retention of drug in the lesion. For example, chitosan with a high molecular weight is an active enhancer.[54] (2) High biocompatibility due to reduced enzymatic and hydrolytic degradation.[55] (3) Controllable *in vivo* drug release achieved by tuning the solubility, pH sensitivity, and zeta potential of the components; and (4) flexibility of conjugated functional chemical groups on the polymer surface for targeting delivery.[56]

2.2.1 Amphiphilic copolymers. Amphiphilic copolymers can assemble into core–shell NPs through the amphiphilic component of hydrophilic and hydrophobic chains. Hydrophobic drugs can be encapsulated into the hydrophobic core to enhance the water solubility of NPs. The outer layer of the hydrophilic shell can promote the stability in plasma, prolong the circulation time, and increase the bioavailability and biosafety of NPs.[57] In Fig. 5, four types of amphiphilic copolymers are discussed, and a brief comparison is presented.

2.2.1.1 Poly(butyl cyanoacrylate)-based NPs. Poly(butyl cyanoacrylate) (PBCA) is a promising delivery system with high adsorption, low toxicity, and good biodegradability. Koffie *et al.* prepared PBCA NPs with spherical and ellipsoid geometry and a mean diameter of 48 nm, and invested their capability for crossing the BBB.[58] As shown in Fig. 6A, Texas Red Glucan dissolved in PBS alone could not penetrate the BBB and remained in the blood vessel at 2 h after intravenous injection. In contrast, after covalently incorporating with Texas Red Glucan and modifying with Tween 80, PBCA NPs could pass through the BBB at 30 min post-intravenous injection and stain amyloid plaques, cerebral amyloid angiopathy, and neuron/glial cell bodies. *In vivo* fluorescence analysis showed that the PBCA NPs crossed the BBB *via* receptor-mediated endocytosis. Most importantly, they did not induce non-specific BBB disruption. However, the use of PBCA NPs is limited due to the generation of toxic hydrolytic by-products (polyacrylic acid and alcohols). Moreover, the pharmacological effects of PBCA NPs were temporary; thus, daily intravenous injection may be required over the course of treatment.[59]

2.2.1.2 Polylactic-acid-based NPs. Polyester polymers, such as polylactic acid (PLA) can produce non-toxic lactic acid and glycolic acid oligomers that can be further degraded into CO_2 and H_2O. Wang *et al.* prepared Cur-encapsulated mPEG-*b*-PLA (NP Cur), which had a smooth surface, a spherical morphology, and a narrow size distribution (147.8 ± 5.7 nm), to effectively deliver Cur to the brain.[60] The Cur-loading efficiency reached as high as 51.7 ± 3.1%. NP Cur can reduce oxidative stress and inflammation by protecting the BBB and inhibiting the activity of M1 microglia. Triphenyltetrazole (TTC) staining was used to evaluate the area and volume of infarct tissue due to inadequate blood supply. In this study, Cur could accumulate to ischemic penumbra at 3 h post-injection. The result showed that the infarct volumes of PBS, Cur, and NP Cur groups were 40.1%, 32.4%, and 18.3%, respectively. Compared with that of the PBS- and Cur-treated groups, the infarct (dead tissue due to inadequate blood supply) volume of the NP Cur-treated group was significantly lower at 3 days after ischemia-reperfusion injury. The data indicated the successful protection of neurons against ischemia-reperfusion injury by NP Cur.

Neuroprotein is a modular transmembrane protein expressed on both angiogenic glioma and endothelial cells; it is a promising receptor for targeted anti-glioma drug delivery. As shown in Fig. 6B, paclitaxel (PTX)-loaded PEG-PLA NPs modified with tLyp-1 peptide (cell penetrating peptides tLyp-1, the ligand of neuroprotein) had a strong affinity to neuroprotein-overexpressed glioma cells; the presence of neuroproteins could significantly enhance the cellular uptake, thus increasing the PTX uptake of the target cells, leading to the inhibition of tumor development.[61] A strong fluorescence signal at the glioma foci indicates that tLyp-1-NP had excellent glioma permeability and targeting ability. In addition, the penetration depth of tLyp-1-NP (121.69 mm) was 1.32-fold higher than that of blank NP (92.02 mm). Compared with NP-PTX (28 days), PTX (23 days), and saline (18 days), tLyp-1-NP-PTX (37 days) could significantly increase the survival time *in vivo*.

2.2.1.3 Poly(lactic-co-glycolic acid)-based NPs. Poly(lactic-*co*-glycolic acid) (PLGA) is formed by random polymerization of lactic and glycolic acids. PLGA has been approved as a pharmaceutical excipient for clinical use by the U.S. Food and Drug Administration.[62]

The formation of extracellular aggregates of Aβ1–42 is a sign of AD.[63,64] It has been reported that Cur not only inhibits the formation of new Aβ aggregates, but also shows anti-amyloid activity by breaking down existing Aβ aggregates.[65] Therefore, Barbara *et al.* prepared Cur-encapsulated PLGA NPs with a loading efficiency of 3% (w/w) and modified them with the g7

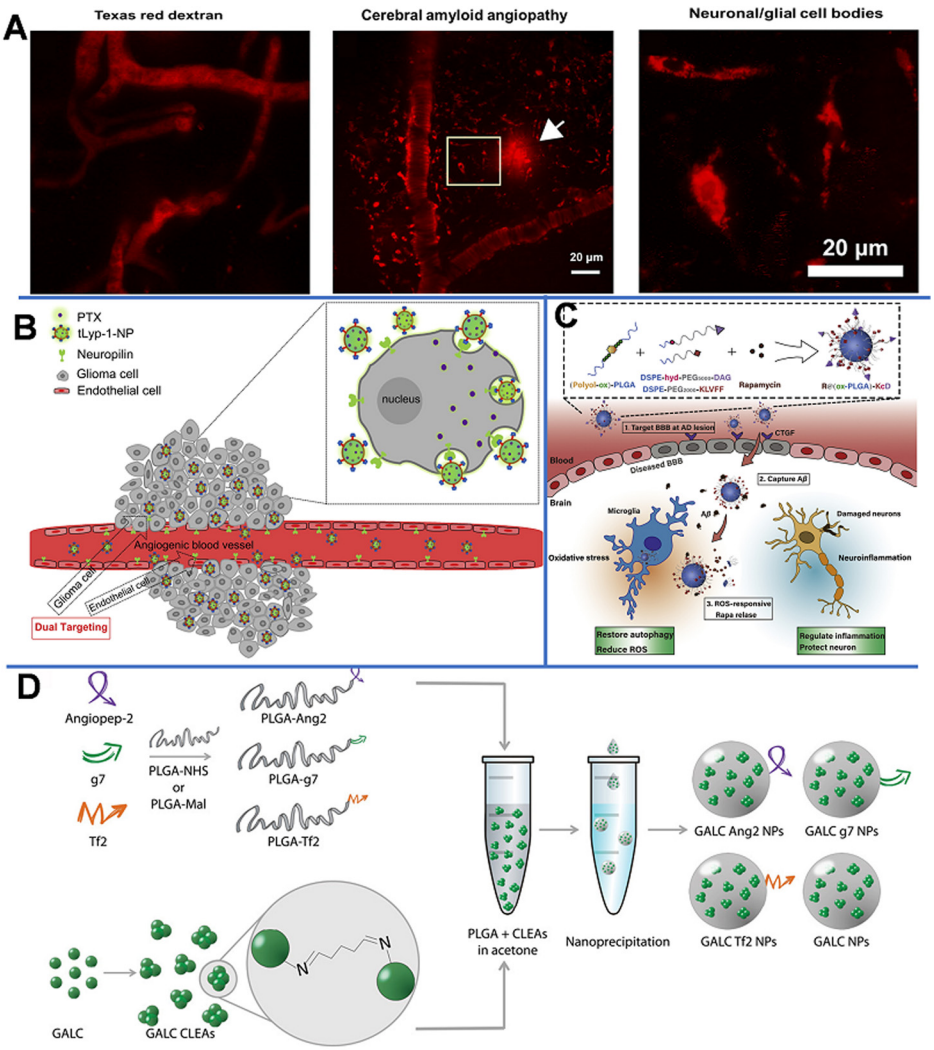

Fig. 6 (A) Texas red glucan is covalently linked to PBCA NPs for BBB penetration and marking the neuropathological changes of AD. Reprinted with permission from ref. 58. Copyright 2011, National Academy of Sciences. (B) tLyp-1-conjugated PEG-PLA NP loaded PTX penetrates the BBB through NRP-mediated endocytosis and permeation. Reprinted with permission from ref. 61. Copyright 2013, Elsevier. (C) Scheme of the ROS-responsive specific targeted R@(ox-PLGA)-KcD. Reprinted with permission from ref. 69. (D) Graphical summary of the synthesis of targeted GALC CLEA NPs. Reprinted with permission from ref. 74. Copyright 2019, Elsevier.

ligand to enhance their BBB penetration capability.[66] It was found that the obtained g7-NPs-Cur could significantly decrease the amount of Aβ aggregates. In another work, by using a high-pressure emulsification-solvent evaporation method, Tsai *et al.* prepared Cur-loaded 163 nm PLGA NPs (C-NPs) with a drug-loading efficiency of 46.9%.[67] With this approach, the retention time of Cur in specific brain areas (the cerebral cortex and hippocampus) was significantly prolonged. Similarly, Bhatt *et al.* synthesized Tet1-peptide-conjugated PLGA-encapsulated nattokinase NPs and found that these NPs can inhibit the formation of Aβ40 plaques in AD and exhibit antifibrinolytic activity.[68] However, due to low drug accumulation in the brain and difficulty in inhibiting the Aβ aggregates, Gao *et al.* designed a nano-cleaner with a rapamycin-loaded ROS-responsive PLGA core and surface modified with KLVFF peptide and acid-cleavable DAG peptide [R@(ox-PLGA)-KcD]. The DGA peptide was an acid-responsive targeting ligand that could be separated from the nano-cleaner to promote transcytosis from endothelial cells into brain parenchyma. The exposed KLVFF could capture Aβ, and in response to the presence of ROS, rapamycin was released to improve Aβ degradation and normalize inflammatory conditions. The physiological evaluation and behavioral experiments in an AD mice model demonstrated the effectiveness and biocompatibility of the nano-cleaner in AD therapy (Fig. 6C).[69]

Cui *et al.* reported magnetic PLGA NPs with transferrin receptor-binding peptide T7 that could co-deliver PTX and Cur.[70] The NPs could increase the drug delivery to the brain by >5 times compared to non-targeting NPs. Furthermore, these NPs could enhance the survival rate compared with free drugs (100% *vs.* 62.5%). In another study by Bi *et al.*, the T7 peptide was used to modify PLGA-PEG micelles.[71] The study revealed that these micelles achieved more efficient accumulation

of the micelles in the brain tumor, providing better tumor inhibition, and better prolonging the survival time compared with the unconjugated counterparts. In addition to the T7 peptide, the iNGR peptide has also been used to functionalize PEG-PLGA NPs and to penetrate gliomas. In this design, the iNGR peptide initially binds to the overexpressed aminopeptidase N in tumors and is then cleaved to CRNGR that could subsequently bind to neuropilin-1 for deep penetration into the tumor parenchyma.[72] Importantly, the size of PLGA NPs can impact the efficiency of drug delivery to the brain. One study has suggested that PLGA NPs with a size of approximately 100 nm could be transported to the brain more efficiently than those with a size of 200 or 800 nm.[73]

Grosso *et al.* developed a new enzyme delivery nanoplatform by encapsulating the cross-linked enzyme aggregate (CLEA) into PLGA NPs, which could encapsulate galactosylceramidase (GALC) and retain good enzyme activity.[74] As shown in Fig. 6D, the obtained NPs were further modified with functional peptides, such as angiopep-2 (ANG-2), g7, or Tf-binding (Tf2) peptides, to enhance the BBB penetration. The *in vitro* study on the transport of NPs in cells and their ability to restore enzyme activity demonstrated that these NPs could effectively deliver GALC into human cells and maintain the enzyme activity up to 96 h. This effective approach provides a promising therapeutic opportunity for lysosomal-storage disorders involving the CNS.

2.2.1.4 Chitosan. Chitosan is obtained by deacetylation of chitin and is broadly utilized in biomedical applications due to the merits of degradability, biocompatibility, good stability, easy synthesis and functions,[75,76] and mucoadhesivity. In 2006, chitosan was approved as a ''generally recognized as safe'' (GRAS) class of natural products by the FDA.

Trapani *et al.* prepared dopamine-encapsulated chitosan NPs to cross the BBB for Parkinson's disease.[77] Gu *et al.* designed double antibody-modified (Tf antibody and bradykinin B2 antibody) chitosan/siRNA NPs (chitosan-NPs) with a spherical shape and an average particle size of 235.7 ± 10.2 nm, which could target HIV-infected brain astrocytes and deliver siRNAs to inhibit HIV replication.[78] Double-ligand modification of NPs is a potential strategy for improving drug-delivery efficiency. Herein, transferrin antibody and bradykinin B2 antibody could specifically bind to transferrin and bradykinin B2 receptors, respectively, and then deliver the siRNA across the BBB into the target cells astrocytes. *In vitro* experimental results demonstrated that this siRNA carrier could effectively silence the expression of the proteins SART3 and hCycT1 proteins related to HIV replication. The knockout rates of SART3 and hCycT1 by chitosan-NPs were 80.9% and 66.6%, respectively.

The deposition of Aβ1–42 peptide aggregates in the brain is a sign of AD. Therefore, amyloid aggregates are widely used as the therapeutic targets in AD. For example, Jha *et al.* studied the anti-amyloidogenic activity of naked chitosan and chitosan-based NPs copolymerized from chitosan and PLGA.[79] The chitosan-based NPs could also break down preformed amyloid fibres derived from the Aβ1–42 peptide. The anti-amyloid activity of chitosan-based NPs was 200-fold stronger than that of PLGA-chitosan-based NPs, and the enhancement was thought to be the surface charge. To improve the efficiency of the drug delivery to the brain, Yang *et al.* synthesized Cur-loaded chitosan-BSA NPs.[80] The encapsulation rate by NPs was measured to be 95.4%. Experimental results showed that chitosan-BSA NPs could improve the BBB-crossing ability of the drug, activate microglia, and stimulate phagocytosis of the Aβ peptide. Recently, Zheng *et al.* applied dihydromyricetin (DMY)-coated Se NPs that were further wrapped by chitosan (which served as a stabilizer) and decorated with the BBB targeting peptide Tg (TGNYKALHPHNG) to yield Tg-CS/DMY@SeNPs for AD treatment.[81] The prepared NPs were sphere with a diameter of less than 50 nm. The results showed that Tg-CS/DMY@SeNPs could successfully cross the BBB to inhibit the aggregation of Aβ and the secretion of inflammatory cytokines involved in the progression of AD. Thus, the Tg-CS/DMY@SeNPs are ideal candidates for AD therapy.

Overall, highly biocompatible polymer-based NPs can enhance brain permeation and tumor accumulation of drugs, and realize the controlled release of drugs under the tumor microenvironment (TME), and thus have been widely used in biomedicine. However, traditional linear polymers face the limitation of a low number of interaction sites and low drug-loading areas. Multi-dimensional polymer-based nanocarriers with abundant active groups and high drug-loading capacity are therefore needed.

2.2.2 Dendrimers. Dendrimers are novel functional polymers with highly branched three-dimensional structures (Fig. 7A). In general, dendrimers consist of an initial core (starting atoms), an inner layer with repeating units, and an outer layer with numerous terminal active groups.[82,83] Dendrimers are greatly advantageous to drug delivery due to their facile surface modification, adjustable molecular weight and shape, good water solubility, and high biocompatibility and biodegradability. Moreover, dendrimers have a passive targeting effect as a result of their enhanced permeability and retention (EPR) effect, which is the characteristic conducive to BBB penetration.[84]

Poly(amidoamine) (PAMAM) contains many cavities that can encapsulate drug molecules, and terminal $-NH_2$ groups that can bind to antibodies and other bioactive substances to form a stable hybrid system.[85] Teow *et al.* prepared a Den-drug complex by conjugating PTX to the surface of PAMAM *via* a glutamate linker.[86] *In vitro* experiments demonstrated that these Den-drug conjugates could cross the endothelial cell monolayers of a porcine brain within 3 h and could be one-way transported (basolateral to apical direction) across the cell monolayers. The prepared G3 PAMAM dendrimers could enhance paracellular transport by opening the tight junctions, thereby successfully delivering the drug into the brain. Conversely, the free drugs could not effectively and unidirectionally permeate the cell monolayers due to the presence of P-gp.

To enhance the drug delivery across the BBB and improve the tumor-targeting delivery efficiency, Li *et al.* constructed a dual brain-targeted drug delivery system (G4-DOX-PEG-Tf) with a hydrodynamic diameter of approximately 19 nm using Tf and tamoxifen (TAM)-modified fourth-generation PAMAM Den that

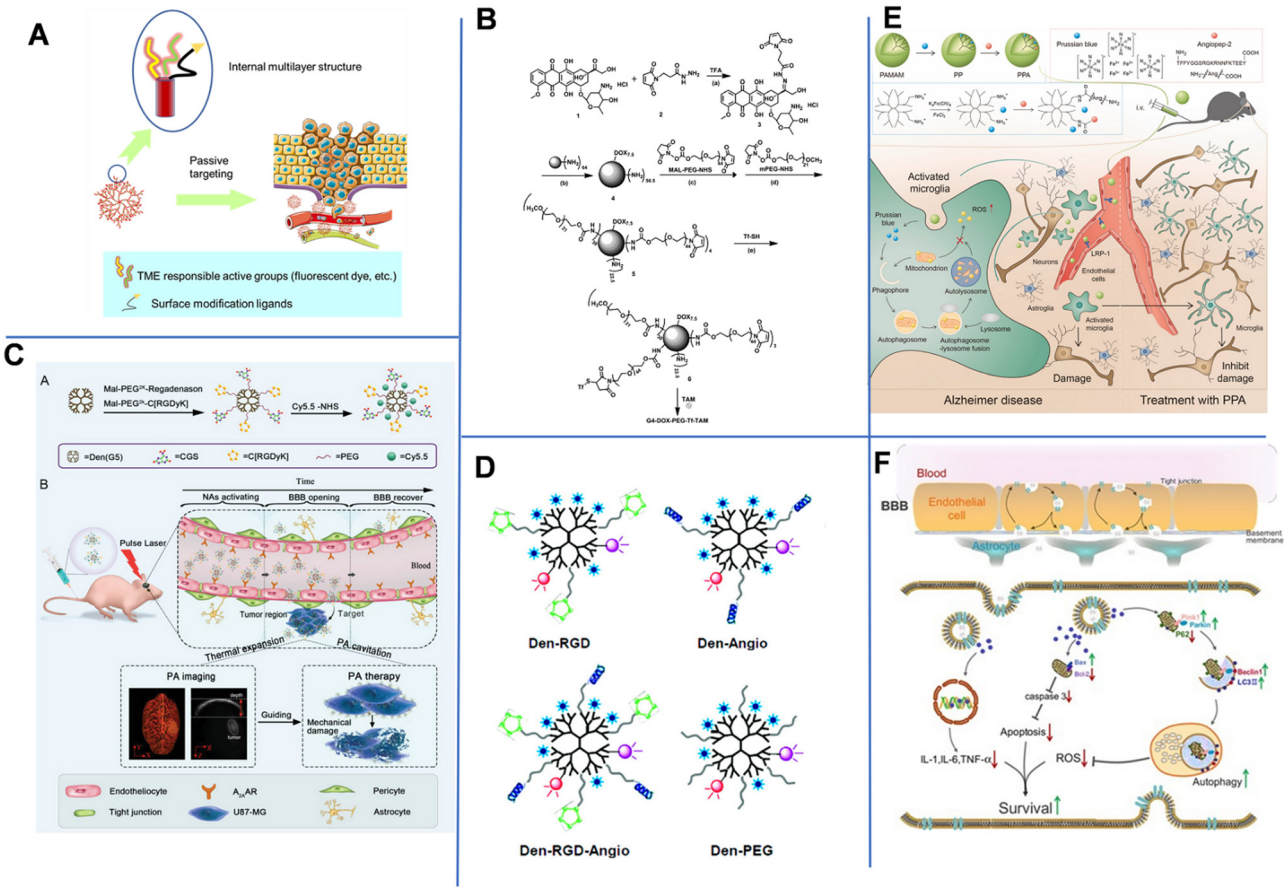

Fig. 7 (A) Schematic diagram of the structure and administration of dendrimers. (B) Synthetic route of the dual-targeting drug carrier. Reprinted with permission from ref. 87. Copyright 2012, Elsevier. (C) Schematic summary of the synthesis and photoacoustic precision glioblastoma therapy of the Dendrimers-RGD/CGS/Cy5.5 (Dendrimers-Den). Reprinted with permission from ref. 90. Copyright 2019, Wiley-VCH. (D) Schematics of the targeted and control nanoprobes. Reprinted with permission from ref. 91. Copyright 2012, American Chemical Society. (E) Illustration of the microglia induced AD microenvironment and mechanisms of regulating the metabolism of microglia.[92] (F) Scheme of the construction of the T-SA-NPs NPs and the potential mechanism of action.[93]

can be used for the treatment of GBM.[87] As shown in Fig. 7B, Den was a pH-sensitive drug vector that could co-load TAM and DOX through pH-sensitive chemical bonds. Additionally, there were one Tf group, seven DOX molecules and over 30 PEG1000 and PEG2000 chains on the surface of one Den molecule. The Tf group improved the BBB-crossing capability, while TAM promoted the accumulation of drug in tumor by inhibiting the efflux transports. In an acidic tumor environment, the pH-sensitive chemical bond was broken, allowing DOX to be released from the system into the tumor tissue. Later, Wang *et al.* demonstrated that conjugating Tf to an intrinsically fluorescent PAMAM could enhance the BBB-crossing ability of nanosystems.[88] Unlike Tf, ANG-2 could effectively enter the brain parenchymal cells through a mechanism mediated by low-density lipoprotein-receptor-related protein-1 (LRP1). Therefore, Huang *et al.* conjugated PAMAM and ANG-2 to a bifunctional PEG, and then hybridized it with pDNA to produce gene-carrying NPs (PAMAM-PEG-ANG/DNA NPs) with a diameter of 110 nm. The NPs could cross the BBB and target glial cells.[89]

In 2019, Liu *et al.* constructed NP-containing PAMAM dendrimers with a diameter of 10 nm. The NPs could cross the BBB through the reorganization of the cytoskeleton of endothelial cells. The NPs were labeled with red-absorbing dye Cy5.5, cyclic [RGDyK] peptide (which targets tumor vasculature and U87-MG glioblastoma cells), and A2AAR agonist agent (CGS) (Fig. 7C).[90] The dendrimers-RGD/CGS/Cy5.5 NPs first target the αvβ3 integrin overexpressed in the blood vessels of brain glioblastoma. The CGS agonist activated A2AAR on vascular endothelial cells to open the BBB, allowing the NPs to enter the glioblastoma. Under pulsed laser irradiation, NPs absorbed the photon energy and generated photoacoustic (PA) shock waves that kill tumor cells. In addition, PA imaging was utilized to clearly locate tumors after Den-RGD/CGS/Cy5.5 administration. A moderate PA signal was detected at the tumor site after 1 h of injection, and the signal gradually increased over time and reached its maximum value at 12 h post-injection.

Magnetic resonance imaging (MRI) is the main approach used in diagnosing brain tumors. Unfortunately, the accuracy of MRI in brain imaging is limited by the short cycle life, non-specificity, and poor BBB permeability of commonly used MRI agents. Yan *et al.* developed a dual-targeting nanoprobe for MRI and optical imaging of brain tumors.[91] As shown in Fig. 7D,

PAMAM-G5 was simultaneously labeled with the tumor-vessel-targeting cyclic (RGDyK) peptide and ANG-2 peptide to produce Den-RGD-Angio with a hydrodynamic diameter of 15.6 nm. The near-infrared (NIR) fluorophore Cy5.5, rhodamine, and the MRI contrast agent Gd^{3+}-DOTA were conjugated to PAMAM-G5. This dual-targeting strategy could achieve targeted delivery of imaging agents to tumors without disturbing or damaging the BBB. With a strong tissue penetration ability of NIR fluorescent agent, the probe could be detected in the brain in real-time within 2 h of injection. *In vivo* imaging results revealed that the Den-RGD-Angio-modified nanoprobe could effectively penetrate the BBB in normal mice, and the tumor boundary could be accurately determined. Similarly, Shi *et al.* constructed Prussian blue/PAMAM dendrimer/Angiopep-2 (PPA) NPs for effective AD treatment. The component PB held ROS scavenging capacity to facilitate mitochondrial autophagy and inhibit amyloid plaques, thus compromise AD. Angiopep-2 had increased the brain-targeted accumulation in the brain. MRI images showed that PPA NPs had a high positive signal after 4 h of injection (Fig. 7E).[92]

Besides, environment-responsive dendrimers are also attractive due to their highly targeted drug delivery, which can avoid systematic toxicity more probably compared to non-responsive dendrimers. In 2020, Du *et al.* constructed $O_2^{\bullet-}$-responsive dendrimers modified with an antioxidant salvianic acid A (SA) and a targeting peptide COG1410 (T-SA-NPs) to aid in BBB crossing when treating ischemic stroke. Fluorescence imaging showed that COG1410-modified NPs conjugated with Texas Red was specifically accumulated in the brain after 6 h of injection (Fig. 7f). Laser confocal microscopy analysis of immunostaining demonstrated the NPs could permeate into the penumbra area of cerebral ischemia. NP-treated mice also showed a better behavioral ability than the control groups.[93] Jin *et al.* prepared a pH-sensitive siLSINCT5-loaded dendrimer tLyp-1 and anti-NKG2A monoclonal antibody (aNKG2A, a checkpoint inhibitor) modified tLyp/aNKNP-siRNA. Once the tLyp/aNKNP-siRNA was targeted and accumulated into the brain, the hydrazone bond between aNKNP and the NPs would be pH-responsively broken and aNKNP released to induce antitumor immunity. Residual NPs were further captured by tumor cells to inhibit the LSINCT5-activated signaling pathways. *In vitro* experiments showed the tLyp/aNKNP-siRNA had a strong anti-proliferation effect. The modification with tLyp-1 endowed the NPs with an excellent BBB-crossing ability. After 24 h of injection, the accumulation of tLyp/aNKNP-siRNA in the brain tumor reached its maximum value.[94]

Dendrimers are a type of nanoscale drug carrier with broad space for development in the field of pharmacy due to their inherent unique advantages. However, the current research on dendrimers is still in the early stages, and the release behavior, targeting ability, and metabolic pathways of drugs need to be further studied both *in vitro* and *in vivo*.

2.3. Biomolecule-based NPs

Biomolecule-based NPs are another type of BBB-crossing nanocarrier that have been widely used. These include engineering and modification of several common biomolecules including proteins, nucleic acids, and virus.

2.3.1 Protein-based NPs. Proteins are fundamental biomacromolecules with high biological activity formed by dehydration condensation of amino acids. Due to the specify and excellent bioactivity, the rapid progress of biotechnology has promoted a series of biomedicine-used proteins by modifying or encapsulating natural or man-made proteins.[95] It has been reported that conjugating drugs with antibodies that could bind to specific receptors on the brain endothelial cells allows for an excellent BBB-crossing capacity of the drugs. Thus, applying ligands for the corresponding receptors as drugs carriers may enhance the accumulation in the brain.[96]

For example, a simple small 12 amino-acid peptide originating from melanotransferrin protein (MTf, belongs to the Tf family) was found to possess improved brain delivery properties.[97] Jefferies *et al.* conjugated MTf with siRNA to construct a peptide-oligonucleotide conjugate (POC) for the therapy of ischemic stroke.[98] Besides, Zhang *et al.* used a high-density lipoprotein-mimicking peptide-phospholipid scaffold (HPPS) to load Cur for the targeted immunomodulation of inflammatory monocytes for further treatment of encephalomyelitis (EVE). The constructed Cur-loaded HPPS (Cur-HPPS) could be internalized specifically by monocytes through the scavenger receptor class B type I (SR-B1) receptor. After incubating for 3 h, over 80% of Cur-HPPS was found to be taken up by monocytes. To make NPs trackable, fluorescent dye DiR-BOA (1,1′-dioctadecyl-3,3,3′,3′-tetramethylindotricarbocyanine iodide bisoleate) was also loaded into the NPs. At 6 and 24 h after injection, a strong fluorescence signal of DiR-BOA was observed in the brain, which was indicative of effective BBB-crossing and brain accumulation (Fig. 8A).[99] To further improve the drug delivery efficiency, Giralt designed the third generation of BBB-shuttles, branched BBB-shuttle peptides. Compared with a single copy of the BBB-shuttle, the branched BBB-shuttle showed higher uptake and improved permeability of the model protein in endothelial cells.[100]

Above all, TME-responsive delivery systems are more attractive approaches. Zuhorn reported dodecamer peptide (G23)-functionalized polydopamine (pD)-coated Cur-loaded zein NPs (CUR-ZpD-G23 NPs) to traverse the BBB in the treatment of glioblastoma. Zein originating from corn could be easily self-assembled into NPs and had a sustained drug release capability. The polydopamine (pD) coating provided NPs with hydrophilicity, colloidal stability, and biocompatibility, and endowed NPs with pH-responsive drug release capability. At pH 7.4, about 45% of Cur was released from CUR-ZpD-G23 NPs, and the released Cur reached up to 80% in 48 h when pH decreased to 5. After incubation for another 8 h, approximately 17% of NPs passed by the *in vitro* BBB model. And the viability of C6 glioma cells incubated with CUR-ZpD-G23 NPs for 48 h dramatically decreased to 25%. All the above results demonstrated the BBB-crossing ability and glioma-treating capacity of NPs.[101] Huang *et al.* constructed an integrin α2β1 targeting ligand (DGEAGGD-GEA) modified with human H-ferritin (HFn) and loaded with DOX (DOX-2D-HFn NPs) for orthotopic glioma therapy. HFn could self-assemble into a cage-like structure that was highly

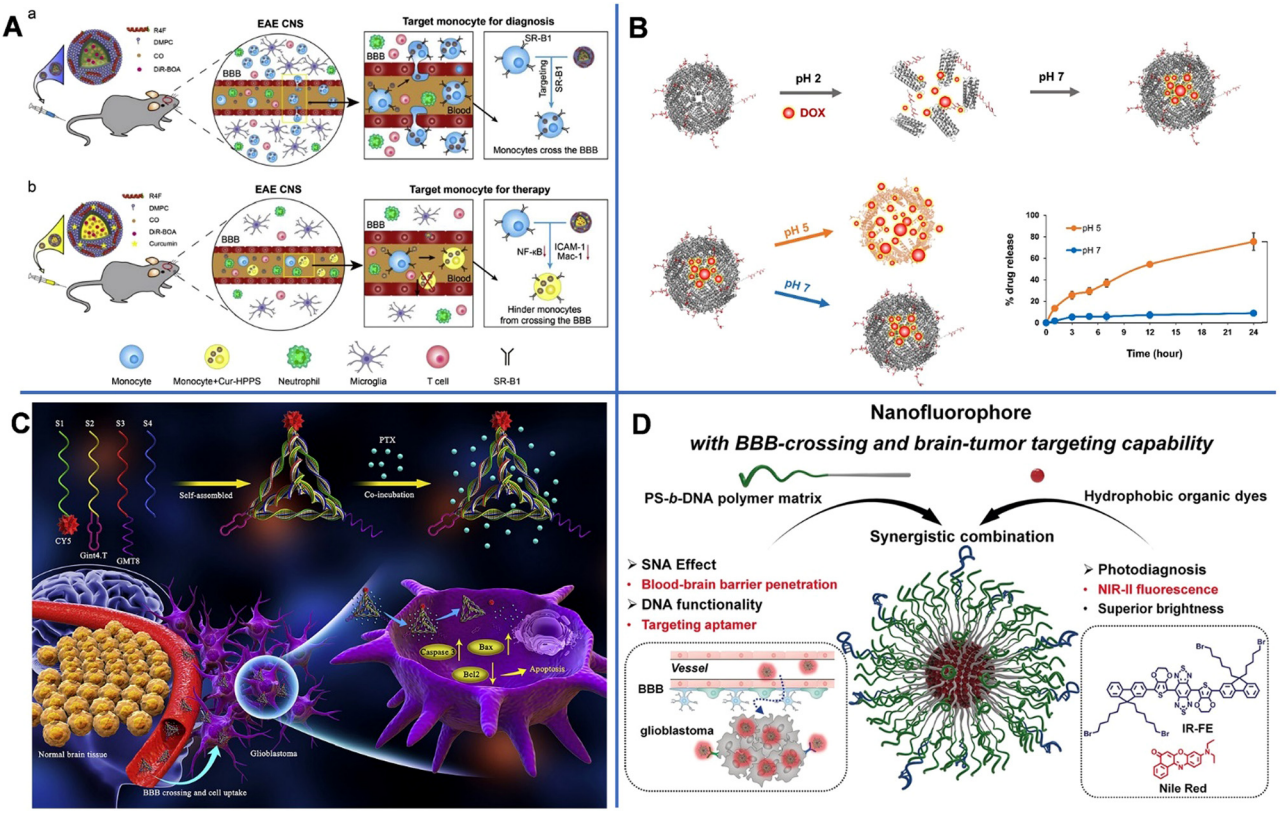

Fig. 8 (A) The design of the HPPS for targeted immunomodulation of inflammatory monocytes.[99] (B) Integrin α2β1-targeting ferritin nanocarrier traverses the blood–brain barrier for effective glioma chemotherapy.[102] (C) The preparation of GPC and the mechanism of GPC inducing apoptosis of U87MG cells *via* crossing the blood–brain barrier and targeting U87MG cells.[120] (D) Illustration of organic fluorescence-emitting spherical nucleic acid self-assembled from PS-*b*-DNA and organic dyes.[121]

tolerant to extreme acidic conditions (pH = 1–2) or extreme basic conditions (pH = 11–13) and high temperatures of up to 80 °C, thus realizing pH-responsive DOX release. At pH 7, only 9% of DOX was released from the NPs after 24 h of incubation, whereas at pH 5, 75% of DOX was released. Besides, the interaction between HFn and TfR1, integrin α2β1 and peptide-DGEAGGDGEA were greatly beneficial to the BBB-crossing capacity of NPs. The amount of integrin α2β1-targeted HFn passed through the BBB and bound to U-87MG cells was almost 2 times higher than that of HFn after four hours of incubation. And the cell toxicity of DOX-2D-HFn (69%) was also 2 times higher than that of free DOX (29%). In an intracranial glioblastoma mouse model, the median survival time of the DOX-2D-HFn NP-treated group was dramatically higher than that of the untreated groups (Fig. 8B).[102]

However, not all proteins are suitable for BBB crossing. Protein-based NPs also face challenges of enzymatic degradation and RES clearance; thus, further surface modification is still required. Gao used erythrocytes (ETm) coating to prevent the loss of nano-drugs after systematic administration.[103]

2.3.2 Virus-based NPs. Virus-based carriers is one of the most important gene transduction tools used for gene therapy. Adeno-associated virus (AAV), a non-enveloped single-strand DNA molecule, has been widely concerned due to the non-pathogenicity, relatively low immunogenicity, and long-lasting expression.[104] But it also faces the limitation of low BBB penetration efficiency due to the immune response[105] that could be compromised by AAV capsid engineering for high transduction or modified with cell penetrating peptides for better cell internalization.

Twelve AAV serotypes from AAV-1 to AAV-12 have been reported,[106] and AAV-9 had the potential to penetrate the BBB and transduce the CNS cells.[107] In 2017, Gradinaru *et al.* reported that AAV-PHP.eB (a variant of the neurotropic vector AAV) could effectively pass through the BBB and could greatly improve the treatment of neurological diseases.[108] Lin *et al.* reported that the ApoE-LDLR pathway was required for intravenous AAV-PHP.eB to penetrate the BBB. Additionally, blood B cells (not T cells) could reduce the transduction of AAV-PHP.eB to the CNS.[109] Wilson *et al.* demonstrated that glycosylphosphatidylinositol (GPI)-linked protein LY6A was involved in BBB transport. There appears to be a direct link between LY6A and AAV-PHP, which held the excellent ability of AAV-PHP to deliver transgenes across the BBB in C57BL/6J mice. Moreover, murine GPI-anchored protein may influence the viral interaction and transcytosis at the BBB.[110]

Besides, Gradinaru *et al.* employed a Cre-transgenic-based screening platform and sequential engineering to engineer

Table 1 Summary of the application of organic-NPs delivery systems in crossing the BBB

Types of nanocarrier	Delivery system	Surface modification	Size (nm)	Drug/gene	Drug loading efficiency	Targets	Diseases	Ref.	Advantages	Disadvantages
Liposome	Phospholipid\CHL	Polyethylene\glucose	100	Coumarin 6	NA	Glucose	NA	23	Biocompatibility; low toxicity; aptitude to trap hydrophilic and lipophilic drugs; prolong drugs' blood circulation time	Limited drug-carrying stability and biological functions; small scale production
	DPPC\DSPC\SPIONs	Cell-penetrating peptide\Anti-GBM antibody	114	DOX	75%	Glioblastoma	Glioma	35		
SLN	Dynasan@114\palmitic acid	83–14 MAb\Tween 80\poloxamer 407\DSPE-PEG(2000)-carboxylic acid	120–450	Saquinavir	79%	α-Subunit;LDLRs	AIDS	39	High monodispersity; long temporal stability; low toxicity; sustained drug release; multi-administration	Limited drug loading capacity; the drug leakage during storage; the storage of solid lipids may form crystals resulting in performance degradation
	Dynasan 116\epikuron 200\short chain alcohols	DPM\ApoE	119	NA	NA	LDLRs	NA	42		
Micelle	CPT–S–S–PEG–COOH	PEG\iRGD peptide	100	CPT\IR780	CPT-11.07	αvβ-Integrin-and neuropilin-1	Glioma	47	Small particle size; flexibility of modification with targeting ligands; prevent or minimize drug degradation; lower adverse side effects; ease of preparation	The degradability of micelles needs to be improved; the probable drug leakage
	Glycol chitosan\stearic acid	TGN peptide	146.2	Cur	76.2%	NA	Glioma	45		
	3-Mercaptopropyl amidine\2-thiolaneimine\ poly(L-lysine)	Glucose\poly(ethylene glycol)-*b*-poly(lysine)	45	ASO	NA	Glut 1	NA	49		
	F-127	F-127	14	Cur	NA	NA	Glioma	46		
	PLGA-lysoGM1	LysoGM1	27.8	DOX	61.6%	NA	Glioma	51		
Amphiphilic copolymer-based NP	PBCA	Tween 80	200	Fluorophores (dextran Trypan blue)\Gadobutrol	NA	LDLRs	AD	58	Controlled drug release; structural controllability; high stability; ease of synthesis; strong drug loading efficiency	Complicated design; poor repeatability
	mPEG-*b*-PLA	mPEG	147.8	Cur	4.92%	NA	Ischemia/ reperfusion	60		
	MePEG-PLA\ male–PEG–PLA	tLyp-1 peptide	111	PTX	NA	Neuroproteins	Glioma	61		
	PLGA	g7	200–250	Cur	60%	NA	AD	66		
	PLGA	Angiopep-2\g7\Tf	200	GALC CLEAs	Angiopep-2(60%)\g7(74%)\Tf (39%)	TfR;LPR-1 receptor	Krabbe disease	74		
	Chitosan	NA	110	Dopamine	81%	NA	Parkinson	77		
Dendrimer	G3-PAMAM	Lauryl chains	13.7	PTX	NA	NA	NA	86	High drug loading efficiency due to the branched structure and internal cavity; adjustable molecular weight and shape; abundant terminal groups for functionalization	Chronic toxicity; poor accumulation *in vivo*
	G4-PAMAM	Tf\TAM	19	DOX	NA	TfR	Glioma	87		
	G5-PAMAM	Cyclic [RGDyK] peptides	10	A_{2A}AR agonis	NA	Integrin	Glioma	90		
	G5-PAMAM	Cyclic [RGDyK] peptide\Angiopep-2 peptides	15.6	NA	NA	Integrin\LPR-1 receptor	Glioma	91		

Table 1 (*continued*)

Types of nanocarrier	Delivery system	Surface modification	Size (nm)	Drug/gene	Drug loading efficiency	Targets	Diseases	Ref.	Advantages	Disadvantages
Virus-based NPs	AAV9	PB5-3 peptide	NA	NA	NA	NA	NA	115	Extensive host cells and high transfection efficiency	Inherent immunogenicity
Protein-based NPs	HPPS	NA	15 ± 2.3	Cur	80 μg mg^{-1}	SR-B1	Encephalomyelitis	99	Biocompatibility, good biodegradability; targeting; easy modification	Enzymic degradation, RES clearance; low drug loading efficiency
	Zein	G23-peptide	<100	Cur	94.4%	NA	Glioma	101		
	HFn	HFn, DGEAGGDGEA peptide	12	DOX	NA	Integrin α2β1, TfR1	Glioma	102		
Nucleic acids-based NPs	tFNA	GMT8, Gint4.T	20	PTX	250 nM	U87MG glioma cells, PDGFRβ	Glioma	120	Excellent biodegradability; adjustable structure and responsible drug-release	
	DNA nanocage	NA	19.7	DOX	15.7	NA	Glioma	122		

AAV-PHP.eB between the surface-exposed AA452 and AA460 in VP3 to develop a variant AAV named AAV.CAP-B10. After intravenous administration, most AAV.CAP-B10 accumulated into the brain, and a small portion accumulates in the liver. The differential accumulation in an adult marmoset was also more distinct compared to that in AAV9 and AAV-PHP.eB.[111]

Although engineered AAV variants have shown success in neuron transduction in preclinical trials, the related animal studies are usually undesirable.[112] Furthermore, small biomolecule modification seems to be a shortcut in the background of the widely used various BBB shuttle peptides in drug delivery.[113,114] Li *et al.* specifically linked AAV9 with PB5-3 peptide (BBB shuttle peptide) to increase its brain accumulation and transduction. Mechanistic studies revealed that the PB5-3 peptide could effectively improve AAV9 trafficking and transcytosis in hCMEC/D3 cells, as well as decrease the clearance of AAV9 from blood.[115]

2.3.3 Nucleic acid-based NPs. Nucleic acids as a natural biomolecule holds the advantages of excellent biocompatibility, biodegradability, and easy functionalization. It can also realize the stimulation triggered release of cargo.[116] Thus, nucleic acid-based nanomaterials have been widely used in *in vivo* applications, including bio-imaging,[117] tumor therapy,[118] multiple detection[119] and nanocarriers. Suitable modification would help to increase the stability and brain accumulation of these nucleic acid-based nanomaterials.

For example, Shi *et al.* utilized two aptamers, GMT8 and Gint4.T conjugated with tetrahedral framework nucleic acid (tFNA) to carry chemotherapeutics PTX (GTG) for treating glioblastomas (Fig. 8C). Both the aptamers had a strong affinity towards platelet-derived growth factor receptor β (PDGFRβ), which is expressed on endothelial cells and is related to tumor progression. Gint4.T was used for targeted delivery. The binding of GMT8 and PDGFRβ would suppress the growth of tumors. The results showed that GTG could effectively permeate the BBB in the *in vitro* BBB model. The migration and invasion inhibition were also significantly observed.[120] Tian *et al.* prepared a block copolymer of DNA and polystyrene-*b*-polyethylene glycol (PS-*b*-PEG) (PS-*b*-DNA) (Fig. 8D) that can self-assemble into 13 nm spherical nucleic acids (SNAs) with the ability to deliver NIR-II dye into the brain (NR@PS-*b*-DNA) and the highest dye-loading amounts of 30 wt%. The NR@PS-*b*-DNA showed 4.5-fold higher traversing efficiency and 3-fold higher accumulation in U87MG cells compared to NR@PS-*b*-PEG. CLSM images of NR@PS-*b*-DNA in coronal slices taken at 3 h post-injection showed prominent fluorescence signals.[121]

More interestingly, Tam *et al.* reported adapt-free and DOX-loaded DNA nanocages produced by supramolecular self-assembly. The nanocages could effectively pass through the BBB *via* endocytosis and be internalized by endothelial cells and U-87 MG cells without peptide modification. The drug-loading efficiency was calculated to be 15.1 ± 2.7%. And the spherical structures held better BBB-crossing than the tubular structures. *In vitro* and *in vivo* experiments demonstrated that the adaptor-free nanocages exhibited less BBB crossing and glioma. Thus, a DNA nanocage-based platform is

a safe and cost-effective tool for targeted drug delivery to the brain.[122]

In summary, virus-based NPs are widespread in gene therapy with extensive host cells and high transfection efficiency. However, inherent immunogenicity can cause the NPs to be easily captured by RES, thus need to be further investigated. The natural receptor-ligand interaction can help in targeting the delivery of protein-based NPs, and components of amino acids can resolve the problem of biosafety. Nucleic acid-functionalized nanomaterials have been widely studied in the field of drug delivery due to their molecular recognition characteristics. Finally, the design of sequences and the use of programmable material can endow NPs with adjustable structures and controlled drug release ability.

In Table 1, we summarize some important examples of organic-NP delivery systems for crossing the BBB.

3. Conclusion and outlook

The use of NP delivery systems in treatment of CNS diseases is particularly important because most free drugs or therapeutic molecules cannot pass through the BBB and be delivered to the brain. Many studies, including many clinical trials, have shown that the drug delivery strategies relying on BBB avoidance rather than facilitating BBB delivery are generally ineffective.[123] Therefore, it is essential to develop effective BBB drug delivery strategies. The development of a NP-delivery system is an innovative and flexible way for delivering drugs to the brain for treating various major diseases. A wide variety of drug delivery systems based on organic NPs (*e.g.*, lipid-, polymer-, and protein-based NPs) have been constructed using suitable carrier materials to achieve effective delivery of anti-tumor drugs.

Generally, all the above-mentioned organic delivery systems exhibit excellent biocompatibility and hold clinical potential. Size, shape, ligand density, lipophilicity and surface chemistry are the main factors for the design of nanocarriers and the selection criteria. For example, smaller NPs can penetrate the BBB more easily than larger NPs, but they are restricted by a smaller surface area and relatively low drug loading amount. Liposomes and SLNs can be used to deliver both hydrophilic and hydrophobic drugs. Micelles are easily prepared, but can only be applied in the delivery of hydrophobic drugs. Polymer-based NPs could avoid the enzymatic and hydrolytic degradation of drugs with a high drug loading efficiency. Amphiphilic copolymers are suitable for hydrophobic drugs. Virus-based nanomedicines are widely used in gene therapy (such as DNA, RNA, and so on), because of their high transfection efficacy. Protein-based NPs, nucleic-based NPs and dendrimers have a number of active groups that can be easily functionalized.

The development of effective nanocarriers requires synergistic improvement of their physicochemical properties and biological functions, in order to broaden their applications in the field of biomedicine. In the optimization of nanomedicines for CNS treatment, it is essential to understand the impact of structures and surface chemical compositions of nanocarriers (*e.g.*, morphology, size, surface functional group, and surface charge) on the BBB-crossing efficiency and safety. Generally, NPs with an average size of approximately 100 nm and neutral and hydrophilic surfaces can be maintained in the blood circulation for a long time and exhibit an improved delivery to tumors.[124] Small-sized NPs may pass through the BBB by endocytosis which is related to the reorganization of the cytoskeleton of endothelial cells.[87] For surface modification, targeting ligands can promote the accumulation of carriers in the brain and enable NPs to cross the BBB *via* different transport mechanisms. Decoration with surfactants is also another plausible approach, as this not only improves the stability of NPs, but can also alter their targeting capacity and increase their cellular uptake. As an example, Tween 80 and F-127 promote the cellular uptake of NPs, while inhibiting P-gp. Other surfactants with similar effects have also been discovered. Although the biosafety of nanomaterials is generally good, their clinical use still has a long way to go.

Although great progress in effective drug delivery to the brain has been achieved by using nano-carriers, further effort is still required to improve their efficacy and safety in clinical use. It is desirable that nanocarriers should have the following characteristics: (1) tumor-targeting properties to promote the targeted delivery of drugs to diseased sites; (2) clinical imaging ability to monitor the delivery, transport, distribution, and clearance of drugs; (3) ability to carry and controllably release different drugs, which is a useful characteristic for combination therapy or therapy in which the drug concentration needs to be in the effective therapeutic window; (4) responsive release mechanism to improve the targeting efficiency and achieve the corresponding results based on the change in the disease sites; (5) ability to effectively cross the BBB without causing irreversible damage; (6) quick degradability and rapid clearance; (7) high safety profiles. While effectiveness in delivering drugs to the CNS and high therapeutic efficacy are important characteristics of nanocarriers, the safety profiles are equally important. NPs have been found to induce brain dysfunction in normal animals and cause oxidative stress and injuries in the brain. To alleviate these problems and facilitate the clinical translation of NPs in the treatment of CNS diseases, various strategies for alleviating the toxicity of NPs have been explored. The neurotoxicity of NPs and the corresponding potential solutions have been described in detail in the literature.[125–129]

It is important to recognize that nanomedicines are being developed to be more effective and safer than ever. With the development of nanotechnology, brain-targeting nanomedicines can be developed for more effective delivery of drugs to the brain. The techniques presented may also have broader applications and be used as a promising platform for the treatment of CNS diseases in the future.

Abbreviations

NA	Not available
Papp	Apparent permeability coefficient

DSPE	1,2-distearoyl-*sn-glycero*-3-phosphotidylethanolamine
SLE	Soya-*a*-lecithin
CHL	Cholesterol
DPPC	1,2-Dipalmitoyl-*sn-glycero*-3-phosphocholine
PEG	Poly ethylene glycol
DHDP	Dihexadecyl phosphate
ApoE	Apolipoprotein E
QU	Quercetin
RA	Rosmarinic acid
AD	Alzheimer's disease
Tf	Transferrin
DSPC	1,2-Distearoyl-*sn-glycero*-3-phosphocholine
SPIONs	Superparamagnetic iron oxide NPs
DOX	Doxorubicin
MAb	Monoclonal antibody
AIDS	Acquired immunodeficiency syndrome
MA	Melanotransferrin antibody
TX/TAM	Tamoxifen
DPM	1,2-Distearoyl-*sn-glycero*-3-phosphoethanolamine-*N*-[maleimide(polyethylene glycol)-2000]
CPT	Camptothecin
iRGD, CRGDRGPDC	Internalizing RGD peptide
ASO	Antisense oligonucleotide
PLGA	Poly(lactic-*co*-glycolic acid)
GM1	Monosialohexylganglioside
PBCA	Poly(butyl cyanoacrylate)
mPEG-*b*-PLA	Poly(ethylene glycol)-*b*-poly(D,L-lactide)
PLA-TPGS	Poly(lactide)-D-α-tocopheryl polyethylene glycol succinate
MePEG-PLA	Methoxypoly(ethylene glycol)3000-poly(lactic acid)34 000
Male–PEG–PLA	Maleimide–poly(ethylene glycol)3400–poly(lactic acid)34 000
PTX	Paclitaxel
SSTR2	Somatostatin receptor 2
g7	Glycopeptide
HAND	HIV-1-associated neurocognitive disorders
GALC CLEAs	Galactosylceramidase cross-linked enzyme aggregate
Cur	Curcumin

Conflicts of interest

There are no conflicts to declare.

Acknowledgements

This work was supported by the National Natural Science Foundation of China (No. 62175262, 81803480), The Science and Technology Innovation Program of Hunan Province (No. 2022RC1201), the Fundamental Research Funds for Central Universities of the Central South University (No. 2020CX021), and the Key R&D Plan of Hunan Province (No. 2022SK2101).

Notes and references

1 J. Hardy and D. J. Selkoe, *Science*, 2002, **297**, 353.
2 J. M. Long and D. M. Holtzman, *Cell*, 2019, **179**, 312.
3 C. Zihni, C. Mills, K. Matter and M. S. Balda, *Nat. Rev. Mol. Cell Biol.*, 2017, **17**, 564–580.
4 S. Ding, A. I. Khan, X. Cai, Y. Song, Z. Lyu, D. Du, P. Dutta and Y. Lin, *Mater. Today*, 2020, **37**, 112–125.
5 M. R. Freeman and D. H. Rowitch, *Neuron*, 2013, **80**, 613–623.
6 R. Daneman, L. Zhou, A. A. Kebede and B. A. Barres, *Nature*, 2010, **468**, 562–566.
7 M. D. Sweeney, K. Kisler, A. Montagne, A. W. Toga and B. V. Zlokovic, *Nat. Neurosci.*, 2018, **21**, 1318.
8 Y. H. Tsou, X. Q. Zhang, H. Zhu, S. Syed and X. Y. Xu, *Small*, 2018, **14**, 1801588.
9 T. P. Heffron, *J. Med. Chem.*, 2016, **59**, 10030.
10 T. Kheirbek and J. L. Pascual, *Curr. Neurol. Neurosci. Rep.*, 2014, **14**, 482.
11 Y. C. Chen, C. F. Chiang, S. K. Wu, L. F. Chen, W. Y. Hsieh and W. L. Lin, *J. Controlled Release*, 2015, **211**, 53.
12 N. U. Barua, S. S. Gill and S. Love, *Brain Pathol.*, 2014, **2**, 117–127.
13 R. Awad, A. Avital and A. Sosnik, *Acta Pharm. Sin. B*, 2022, DOI: **10.1016/j.apsb.2022.07.003**.
14 C. Ferraris, R. Cavalli, P. P. Panciani and L. Battaglia, *Int. J. Nanomed.*, 2020, **15**, 2999.
15 M. Nowak, M. E. Helgeson and S. Mitragotri, *Adv. Ther.*, 2020, **3**, 1900073.
16 Y. H. Tsou, X. Q. Zhang, H. Zhu, S. Syed and X. Y. Xu, *Small*, 2017, **13**, 1701921.
17 D. Furtado, M. Bjornmalm, S. Ayton, A. I. Bush, K. Kempe and F. Caruso, *Adv. Mater.*, 2018, **30**, 1801362.
18 J. B. Xie, Z. Y. Shen, Y. Anraku, K. Kataoka and X. Y. Chen, *Biomaterials*, 2019, **224**, 119491.
19 E. Rideau, R. Dimova, P. Schwille, F. R. Wurm and K. Landfester, *Chem. Soc. Rev.*, 2018, **47**, 8572.
20 M. Agrawal, Ajazuddin, D. K. Tripathi, S. Saraf, S. Saraf, S. G. Antimisiaris, S. Mourtas, M. Hammarlund-Udenaes and A. Alexander, *J. Controlled Release*, 2017, **260**, 61.
21 C. Ross, M. Taylor, N. Fullwood and D. Allsop, *Int. J. Nanomed.*, 2018, **13**, 8507.
22 R. Alyautdin, I. Khalin, M. I. Nafeeza, M. H. Haron and D. Kuznetsov, *Int. J. Nanomed.*, 2014, **9**, 795.
23 F. L. Xie, N. Yao, Y. Qin, Q. Y. Zhang, H. L. Chen, M. Q. Yuan, J. Tang, X. K. Li, W. Fan, Q. Zhang, Y. Wu, L. Hai and Q. He, *Int. J. Nanomed.*, 2012, **7**, 163.
24 Y. Zhang, H. Qu and X. Xue, *Biomater. Sci.*, 2022, **10**, 423.
25 Y. Y. Zhang, L. Zhang, Y. Hu, K. Jiang, Z. Q. Li, Y.-Z. Lin, G. Wei and W. Y. Lu, *J. Controlled Release*, 2018, **289**, 102.
26 G. Sharma, A. Modgil, B. Layek, K. Arora, C. W. Sun, B. Law and J. Singh, *J. Controlled Release*, 2013, **167**, 1.

27 L. Kong, X. Li, Y. Ni, H. Xiao, Y. Yao, Y. Wang, R. Ju, H. Li, J. Liu, M. Fu, Y. Wu, J. Yang and L. Cheng, *Int. J. Nanomed.*, 2020, **15**, 2841–2858.
28 O. A. Marcos-Contreras, C. F. Greineder, R. Y. Kiseleva, H. Parhiza, L. R. Walsh, V. Z. Ramirez, J. W. Myerson, E. D. Hood, C. H. Villa, I. Tombacz, N. Pardi, A. Seliga, B. L. Mui, Y. K. Tam, P. M. Glassman, V. V. Shuvaev, J. Nong, J. S. Brenner, M. Khoshnejad, T. Madden, D. Weissmann, Y. Persidsky and V. R. Muzykantov, *Proc. Natl. Acad. Sci. U. S. A.*, 2020, **117**, 3405–3414.
29 B. D. S. Rodrigues, H. Oue, A. Banerjee, T. Kanekiyo and J. Singh, *J. Controlled Release*, 2018, **286**, 264.
30 S. Lakkadwala, B. D. S. Rodrigues, C. W. Sun and J. Singh, *J. Controlled Release*, 2019, **307**, 247.
31 Y. Z. Zhao, B. X. Shen, X. Z. Li, M. Q. Tong, P. P. Xue, R. Chen, Q. Yao, B. Chen, J. Xiao and H. L. Xu, *Nanoscale*, 2020, **12**, 15473.
32 A. Papachristodoulou, R. D. Signorell, B. Werner, D. Brambilla, P. Luciani, M. Cavusoglu, J. Grandjean, M. Silginer, M. Rudin, E. Martin, M. Weller, P. Roth and J.-C. Leroux, *J. Controlled Release*, 2019, **295**, 130.
33 C. Y. Lin, Y. C. Lin, C. Y. Huang, S. R. Wu, C. M. Chen and H. L. Liu, *J. Controlled Release*, 2020, **321**, 519.
34 A. L. Bredlau, A. Motamarry, C. Chen, M. A. McCrackin, K. Helke, K. E. Armeson, K. Bynum, A. M. Broome and D. Haemmerich, *Drug Delivery*, 2018, **25**, 973.
35 D. Shi, G. J. Mi, Y. Shen and T. J. Webster, *Nanoscale*, 2019, **11**, 15057.
36 C. Tapeinos, M. Battaglini and G. Ciofani, *J. Controlled Release*, 2017, **264**, 306.
37 P. F. Zhao, Z. C. Le, L. X. Liu and Y. M. Chen, *Nano Lett.*, 2020, **20**, 5415.
38 Y. Zhao, Y. X. Chang, X. Hu, C. Y. Liu, L. H. Quan and Y. H. Liao, *Int. J. Pharm.*, 2017, **516**, 364.
39 Y. C. Kuo and H. F. Ko, *Biomaterials*, 2013, **34**, 4818.
40 G. Graverini, V. Piazzini, E. Landucci, D. Pantano, P. Nardiello, F. Casamenti, D. E. Pellegrini-Giampietro, A. R. Bilia and M. C. Bergonzi, *Colloids Surf., B*, 2018, **161**, 302–313.
41 G. R. Topal, M. Mészáros, G. Porkoláb, A. Szecskó, T. F. Polgár, L. Siklós, M. A. Deli, S. Veszelka and A. Bozkir, *Pharmaceutics*, 2022, **13**, 38.
42 R. D. Magro, F. Ornaghi, I. Cambianica, S. Beretta, F. Re, C. Musicanti, R. Rigolio, E. Donzelli, A. Canta, E. Ballarini, G. Cavaletti, P. Gasco and G. Sancini, *J. Controlled Release*, 2017, **249**, 103.
43 H. Cabralnull, K. Miyatanull, K. Osadanull and K. Kataoka, *Chem. Rev.*, 2018, **118**, 6844.
44 Y. P. Li, K. Xiao, W. Zhu, W. B. Deng and K. S. Lam, *Adv. Drug Delivery Rev.*, 2014, **66**, 58.
45 S. M. Vasudevan, N. Ashwanikumar and G. S. V. Kumar, *Biomater. Sci.*, 2019, **7**, 4017.
46 A. Singh, W. Kim, Y. Kim, K. Jeong, C. S. Kang, Y. Kim, J. Koh, S. D. Mahajan, P. N. Prasad and S. Kim, *Adv. Funct. Mater.*, 2016, **26**, 7057.
47 L. Lu, X. J. Zhao, T. W. Fu, K. Li, Y. He, Z. Luo, L. L. Dai, R. Zeng and K. Y. Cai, *Biomaterials*, 2020, **230**, 119666.
48 C. Rinaldi and M. J. A. Wood, *Nat. Rev. Neurol.*, 2018, **14**, 9.
49 H. S. Min, H. J. Kim, M. Naito, S. Ogura, K. Toh, K. Hayashi, B. S. Kim, S. Fukushima, Y. Anraku, K. Miyata and K. Kataoka, *Angew. Chem., Int. Ed.*, 2020, **59**, 8173.
50 R. W. Ledeen and G. Wu, *Trends Biochem. Sci.*, 2015, **40**, 407.
51 Y. Yin, J. Wang, M. Yang, R. L. Du, G. Pontrelli, S. McGinty, G. X. Wang, T. Y. Yin and Y. Z. Wang, *Nanoscale*, 2020, **12**, 2946–2960.
52 Y. F. Lu, C. Li, Q. J. Chen, P. X. Liu, Q. Guo, Y. Zhang, X. L. Chen, Y. J. Zhang, W. X. Zhou, D. H. Liang, Y. W. Zhang, T. Sun, W. G. Lu and C. Jiang, *Adv. Mater.*, 2019, **31**, 1808361.
53 Y. F. Lu, Z. Y. Guo, Y. J. Zhang, C. Li, Y. Zhang, Q. Guo, Q. J. Chen, X. L. Chen, X. He, L. S. Liu, C. H. Ruan, T. Sun, B. Ji, W. G. Lu and C. Jiang, *Adv. Sci.*, 2018, **6**, 1801586.
54 N. G. Schipper, K. M. Vårum and P. Artursson, *Pharm. Res.*, 1996, **13**, 16861692.
55 Y. Chen and L. Liu, *Adv. Drug Delivery Rev.*, 2012, **64**, 640–665.
56 T. Patel, J. B. Zhou, J. M. Piepmeier and W. M. Saltzman, *Adv. Drug Delivery Rev.*, 2012, **64**, 701.
57 X. Guo, L. Wang, X. Wei and S. Zhou, *J. Polym. Sci. Pol. Chem.*, 2016, **54**, 3525–3550.
58 R. M. Koffie, C. T. Farrar, L. J. Saidi, C. M. William, B. T. Hyman and T. L. Spires-Jones, *Proc. Natl. Acad. Sci. U. S. A.*, 2011, **108**, 18837.
59 A. Friese, E. Seiller, G. Quack, B. Lorenz and J. Kreuter, *Eur. J. Pharm. Biopharm.*, 2000, **49**, 103.
60 Y. Wang, J. Luo and S. Y. Li, *ACS Appl. Mater. Interfaces*, 2019, **11**, 3763.
61 Q. Y. Hu, X. L. Gao, G. Z. Gu, T. Kang, Y. F. Tu, Z. Y. Liu, Q. X. Song, L. Yao, Z. Q. Pang, X. G. Jiang, H. Z. Chen and J. Chen, *Biomaterials*, 2013, **34**, 5640.
62 Q. Chen, J. W. Chen, Z. J. Yang, J. Xu, L. G. Xu, C. Liang, X. Han and Z. Liu, *Adv. Mater.*, 2019, **31**, 1802228.
63 A. W. P. Fitzpatrick, B. Falcon, S. He, A. G. Murzin, G. Murshudov, H. J. Garringer, R. A. Crowther, B. Ghetti, M. Goedert and S. H. W. Scheres, *Nature*, 2017, **547**, 185.
64 W. Qiang, W. M. Yau, J.-X. Lu, J. Collinge and R. Tycko, *Nature*, 2017, **541**, 217.
65 S. N. Fan, Y. Q. Zheng, X. Liu, W. L. Fang, X. Y. Chen, W. Liao, X. N. Jing, M. Lei, E. X. Tao, Q. L. Ma, X. M. Zhang, R. Guo and J. Liu, *Drug Delivery*, 2018, **25**, 1091.
66 R. Barbara, D. Belletti, F. Pederzoli, M. Masoni, J. Keller, A. Ballestrazzi, M. A. Vandelli, G. Tosi and A. M. Grabrucker, *Int. J. Pharm.*, 2017, **526**, 413.
67 Y. M. Tsai, C. F. Chiena, L. C. Lina and T.-H. Tsai, *Int. J. Pharm.*, 2011, **416**, 331.
68 P. C. Bhatt, A. Verma, F. A. Al-Abbasi, F. Anwar, V. Kumar and B. P. Panda, *Int. J. Nanomed.*, 2017, **12**, 8749.
69 T. Lei, Z. Yang, X. Xia, Y. Chen, X. Yang, R. Xie, F. Tong, X. Wan and H. Gao, *Acta Pharm. Sin. B*, 2021, **11**, 4032–4044.
70 Y. N. Cui, M. Zhang, F. Zeng, H. Y. Jin, Q. Xu and Y. Z. Huang, *ACS Appl. Mater. Interfaces*, 2016, **8**, 32159.

71 Y. K. Bi, L. S. Liu, Y. F. Lu, T. Sun, C. Shen, X. L. Chen, Q. J. Chen, S. An, X. He, C. H. Ruan, Y. H. Wu, Y. J. Zhang, Q. Guo, Z. X. Zheng, Y. H. Liu, M. Q. Lou, S. G. Zhao and C. Jiang, *ACS Appl. Mater. Interfaces*, 2016, **8**, 27465.
72 T. Kang, X. L. Gao, Q. Y. Hu, D. Jiang, X. Y. Feng, X. Zhang, Q. X. Song, L. Yao, M. Huang, X. G. Jiang, Z. Q. Pang, H. Z. Chen and J. Chen, *Biomaterials*, 2014, **35**, 4319.
73 L. J. Cruz, M. A. Stammes, I. Que, E. Rv Beek, V. T. Knol-Blankevoort, T. J. A. Snoeks, A. Chan, E. L. Kaijzel and C. W. G. M. Lowik, *J. Controlled Release*, 2016, **223**, 31.
74 A. D. Grosso, M. Gallianil, L. Angella, M. Santi, I. Tonazzini, G. Parlanti, G. Signore and M. Cecchini, *Sci. Adv.*, 2019, **5**, eaax7462.
75 M. N. V. R. Kumar, R. A. A. Muzzarelli, C. Muzzarelli, H. Sashiwa and A. J. Domb, *Chem. Rev.*, 2004, **104**, 6017.
76 S. W. Yu, X. L. Xu, J. F. Feng, M. Liu and K. L. Hu, *Int. J. Pharm.*, 2019, **560**, 282.
77 A. Trapani, E. D. Giglio, D. Cafagna, N. Denora, G. Agrimi, T. Cassano, S. Gaetani, V. Cuomo and G. Trapani, *Int. J. Pharm.*, 2011, **419**, 296.
78 J. J. Gu, K. Al-Bayati and E. A. Ho, *Drug Delivery Transl. Res.*, 2017, **7**, 497.
79 A. Jha, V. Ghormade, H. Kolge and K. M. Paknikar, *J. Mater. Chem. B*, 2019, **7**, 3362.
80 R. Yang, Y. Zheng, Q. J. Wang and L. Zhao, *Nanoscale Res. Lett.*, 2018, **13**, 330.
81 L. Yang, Y. Cui, H. Liang, Z. Li, N. Wang, Y. Wang and G. Zheng, *ACS Appl. Mater. Interfaces*, 2022, **14**(27), 30557–30570.
82 S. Mignani, J. Rodrigues, H. Tomas, M. Zablocka, X. Y. Shi, A. M. Caminade and J.-P. Majoral, *Chem. Soc. Rev.*, 2018, **47**, 514.
83 H. He, Y. Li, X.-R. Jia, J. Du, X. Ying, W.-L. Lu, J.-N. Lou and Y. Wei, *Biomaterials*, 2011, **32**, 478.
84 V. Leiro, S. D. Santos, C. D. F. Lopes and A. P. Pego, *Adv. Funct. Mater.*, 2018, **28**, 1700313.
85 J. Li, H. M. Liang, J. Liu and Z. Y. Wang, *Int. J. Pharm.*, 2018, **546**, 215.
86 H. M. Teow, Z. Y. Zhou, M. Najlah, S. R. Yusof, N. J. Abbott and A. D'Emanuele, *Int. J. Pharm.*, 2013, **441**, 701.
87 Y. Li, H. He, X. R. Jia, W.-L. Lu, J. N. Lou and Y. Wei, *Biomaterials*, 2012, **33**, 3899.
88 G. Y. Wang, X. W. Zhao, H. G. Wu, D. B. Lovejoy, M. Zheng, A. Lee, L. B. Fu, K. T. Miao, Y. An, N. Sayyadi, K. J. Ding, R. S. Chung, Y. Q. Lu, J. Li, M. Morsch and B. Y. Shi, *Small*, 2020, **16**, 2003654.
89 S. X. Huang, J. F. Li, L. Han, S. H. Liu, H. J. Ma, R. Q. Huang and C. Jiang, *Biomaterials*, 2011, **32**, 6832.
90 L. M. Liu, Q. Chen, L. W. Wen, C. Li, H. Qin and D. Xing, *Adv. Funct. Mater.*, 2019, **29**, 1808601.
91 H. H. Yan, L. Wang, J. Y. Wang, X. F. Weng, H. Lei, X. X. Wang, L. Jiang, J. H. Zhu, W. Y. Lu, X. B. Wei and C. Li, *ACS Nano*, 2012, **6**, 410.
92 G. Zhong, H. Long, T. Zhou, Y. Liu, J. Zhao, J. Han, X. Yang, Y. Yu, F. Chen and S. Shi, *Biomaterials*, 2022, **288**, 121690.
93 Y. Li, X. Zhang, Z. Qi, X. Guo, X. Liu, W. Shi, Y. Liu and L. Du, *Nano Res.*, 2020, **13**, 2791–2802.
94 Z. Jin, L. Piao, G. Sun, C. Lv, Y. Jing and R. Jin, *J. Drug Targeting*, 2021, **29**, 323–335.
95 Z. Haidar, R. Hamdy and M. Tabrizian, *Biomaterials*, 2008, **29**, 1207–1215.
96 W. A. Jefferies, M. R. Brandon, S. V. Hunt, A. F. Williams, K. C. Gatter and D. Y. Mason, *Nature*, 1984, **312**, 162–163.
97 G. Thom, M. Tian, J. P. Hatcher, N. Rodrigo, M. Burrell, I. Gurrell, T. Z. Vitalis, T. Abraham, W. A. Jefferies, C. I. Webster and R. Gabathuler, *J. Cereb. Blood Flow Metab.*, 2019, **39**, 2074–2088.
98 B. A. Eyford, C. S. B. Singh, T. Abraham, L. Munro, K. B. Choi, T. Hill, R. Hildebrandt, I. Welch, T. Z. Vitalis, R. Gabathuler, J. A. Gordon, H. Adomat, E. S. T. Guns, C. Lu, C. G. Pfeifer, M. Tian and W. A. Jefferies, *Front. Mol. Biosci.*, 2021, **8**, 611367.
99 L. Lu, S. Qi, Y. Chen, H. Luoa, S. Huang, X. Yu, Q. Lu and Z. Zhang, *Biomaterials*, 2020, **245**, 119987.
100 D. P. Cristina, O. S. Benjam, S. N. Macarena, T. Meritxell and G. Ernest, *Chem. Sci.*, 2018, **9**, 8409–8415.
101 H. Zhang, W. L. van Os, X. Tian, G. Zu, L. Ribovski, R. Bron, J. Bussmann, A. Kros, Y. Liu and I. S. Zuhorn, *Biomater. Sci.*, 2021, **9**, 7092–7103.
102 C. Huang, C. Chuang, Y. Chen, H. Wang, J. Lin, C. Huang, K. Wei and F. Huang, *J. Nanobiotechnol.*, 2021, **19**, 180.
103 C. Gao, W. Gong, M. Yang, X. Chu, Y. Wang, Z. Li, Y. Yang and C. Gao, *J. Drug Targeting*, 2020, **28**, 1085–1095.
104 G. Massaro, C. N. Z. Mattar, A. M. S. Wong, E. Sirka, S. M. K. Buckley, B. R. Herbert, S. Karlsso, D. P. Perocheau, D. Burke, S. Heales, A. Richard-Londt, S. Brandner, M. Huebecker, D. A. Priestman, F. M. Platt, K. Mills, A. Biswas, J. D. Cooper, J. K. Y. Chan, S. H. Cheng, S. N. Waddington and A. A. Rahim, *Nat. Med.*, 2018, **24**, 1317–1323.
105 D. Blessing and N. Déglon, *Curr. Opin. Virol.*, 2016, **21**, 61–66.
106 P. Colella, G. Ronzitti and F. Mingozzi, *Mol. Ther.–Methods Clin. Dev.*, 2017, **8**, 87–104.
107 H. Fu, J. Dirosario, S. Killedar, K. Zaraspe and D. M. McCarty, *Mol. Ther.*, 2011, **19**, 1025–1033.
108 K. Y. Chan, M. J. Jang, B. B. Yoo, A. Greenbaum, N. Ravi, W. Wu, L. S. Guardado, C. Lois, S. K. Mazmanian, B. E. Deverman and V. Gradinaru, *Nat. Neurosci.*, 2017, **20**, 1172–1179.
109 B. Xie, X. Wang, Y. Pan, G. Jiang, J. Feng and Y. Lin, *Theranostics*, 2021, **11**, 1177–1191.
110 J. Hordeaux, Y. Yuan, P. M. Clark, Q. Wang, R. A. Martino, J. J. Sims, P. Bell, A. Raymond, W. L. Stanford and J. M. Wilson, *Mol. Ther.*, 2019, **27**, 912–921.
111 D. Goertsen, N. C. Flytzanis, N. Goeden, M. R. Chuapoco, A. Cummins, Y. Chen, Y. Fan, Q. Zhang, J. Sharma, Y. Duan, L. Wang, G. Feng, Y. Chen, N. Y. Ip, J. Pickel and V. Gradinaru, *Nat. Neurosci.*, 2022, **25**, 106.
112 J. Hordeaux, Q. Wang, N. Katz, E. L. Buza, P. Bell and J. M. Wilson, *Mol. Ther.*, 2018, **26**, 664–668.

113 C. Chen, Z. Duan, Y. Yuan, R. Li, L. Pang, J. Liang, X. Xu and J. Wang, *ACS Appl. Mater. Interfaces*, 2017, **9**, 5864–5873.
114 B. Zhang, X. Sun, H. Mei, Y. Wang, Z. Liao, J. Chen, Q. Zhang, Y. Hu, Z. Pang and X. Jiang, *Biomaterials*, 2013, **34**, 9171–9182.
115 X. Zhang, Z. Chai, A. L. Dobbins, M. S. Itano, C. Askew, Z. Miao, H. Niu, R. J. Samulski and C. Li, *Biomaterials*, 2022, **281**, 121340.
116 P. K. Lo, P. Karam, F. A. Aldaye, C. K. McLaughlin, G. D. Hamblin, G. Cosa and H. F. Sleiman, *Nat. Chem.*, 2010, **2**, 319–328.
117 D. Jiang, Y. Sun, J. Li, Q. Li, M. Lv, B. Zhu, T. Tian, D. Cheng, J. Xia, L. Zhang, L. Wang, Q. Huang, J. Shi and C. Fan, *ACS Appl. Mater. Interfaces*, 2016, **8**, 4378–4384.
118 K. R. Kim, D. Bang and D. R. Ahn, *Biomater. Sci.*, 2016, **4**, 605–609.
119 N. Li, M. Wang, X. Gao, Z. Yu, W. Pan, H. Wang and B. Tang, *Anal. Chem.*, 2017, **89**, 6670–6677.
120 S. Shi, W. Fu, S. Lin, T. Tian, S. Li, X. Shao, Y. Zhang, T. Zhang, Z. Tang, Y. Zhou, Y. Lin and X. Cai, *Nanomedicine*, 2019, **21**, 102061.
121 F. Xiao, L. Lin, Z. Chao, C. Shao, Z. Chen, Z. Wei, J. Lu, Y. Huang, L. Li, Q. Liu, Y. Liang and L. Tian, *Angew. Chem., Int. Ed.*, 2020, **5**, 9702–9710.
122 D. Y. Tam, J. W. Ho, M. S. Chan, C. H. Lau, T. J. H. Chang, H. M. Leung, L. S. Liu, F. Wang, L. L. H. Chan, C. Tin and P. K. Lo, *ACS Appl. Mater. Interfaces*, 2020, **12**, 28928–28940.
123 W. M. Pardridge, *Front. Aging Neurosci.*, 2020, **11**, 373.
124 S. D. Li and L. Huang, *Mol. Pharmaceutics*, 2008, **5**, 496.
125 Z. Yang, Z. W. Liu, R. P. Allaker, P. Reip, J. Oxford, Z. Ahmad and G. Ren, *J. R. Soc., Interface*, 2010, **7**, S411.
126 C. Vinod and S. Jena, *Front. Pharmacol.*, 2021, **12**, 612692.
127 Y. Hu and J. Gao, *Int. J. Pharm.*, 2010, **394**, 115.
128 A. B. Engin and A. Engin, *Prog. Brain Res.*, 2019, **245**, 281.
129 Q. Du, D. Ge, V. Mirshafiee, C. Chen, M. Li, C. Xue, X. Maab and B. Sun, *Nanoscale*, 2019, **11**, 12965.